Coordination Chemistry Reviews 255 (2011) 1293–1318

Contents lists available at ScienceDirect

Coordination Chemistry Reviews

journal homepage: www.elsevier.com/locate/ccr

Review

Single-source precursors to gallium and indium oxide thin films

Leanne G. Bloor, Claire J. Carmalt*, David Pugh

Department of Chemistry, University College London, Christopher Ingold Laboratories, 20 Gordon St, London WC1H 0AJ, UK

Contents

ARTICLE INFO

Article history:
Received 31 August 2010
Accepted 15 December 2010
Available online 23 December 2010

Keywords:
Gallium oxide
Indium oxide
Single-source precursors

ABSTRACT

Gallium and indium oxide thin films have received much attention in recent years for their wide range of applications. This review summarises the literature concerning single-source precursors and the methods employed to deposit gallium and indium oxide thin films using these compounds. An update of the literature outlining compounds which are potential single-source precursors to these materials is also included.

1. Introduction

In recent years, due to their wide range of applications, there has been a huge interest in the production of gallium and indium oxide thin films [1]. A variety of methods to deposit these films exists, as do a large selection of well-defined molecular compounds which contain a preformed M–O bond (M = Ga, In) that can be used in deposition processes without an additional oxygen input: these are called single-source precursors [2]. Single-source precursors are ideal for producing gallium and indium oxide thin films because they provide a simple and clean route to these materials, thus eliminating the need for a mixture of precursors which can often be toxic and/or expensive, as well as involving complicated gas-phase reaction dynamics which can result in the formation of non-stoichiometric films [3].

Gallium oxide (Ga_2O_3) thin films are semiconducting above 500 °C and act as a gas sensor for reducing gases (e.g. CO, CO_2, EtOH) [4,5]. Above 900 °C, they can detect the concentration of oxygen present in a system and therefore the function of the gas

* Corresponding author.
E-mail address: c.j.carmalt@ucl.ac.uk (C.J. Carmalt).

0010-8545/$ – see front matter © 2011 Elsevier B.V. All rights reserved.
doi:10.1016/j.ccr.2010.12.018

sensor could be switched from reducing gases to oxidising gases when using gallium oxide [6–8]. Oxygen gas sensors have practical use in monitoring and controlling oxygen concentrations in waste gases, chemical processes and exhaust gases of automobiles. Gallium oxide films also have potential practical uses outside of sensors, such as a white-light-emitting luminophore [9,10], as solid electrolytes (mostly $LaGaO_3$ doped with various metals) [11] and in zeolite catalytic systems [12].

Indium oxide (In_2O_3) thin films are conductive, transparent to visible light and are used as a transparent conducting oxide (TCO); these have important applications in optoelectronic devices, e.g. display panels and solar cell windows. In_2O_3 nanorods have also been reported to have sensing properties to formaldehyde [13]. Additionally, In_2O_3-modified gallium oxide thin films have been reported to be sensitive to ozone concentration [14]: in contrast, doping indium oxide with gallium greatly improves the conductivity of the overall film [15,16].

These group 13 oxide films can also be doped with other elements to change the properties of the films. Tin-doped indium oxide (ITO) is one of the most widely used TCOs [17], since tin doping increases the conductivity of the overall film without loss of transparency [18]. Other elements have also been incorporated into indium oxide to increase its conductivity, including fluorine [19] and sulfur [20]. Nitrogen-doped In_2O_3 thin films have been reported as visible light photocatalysts: upon doping with nitrogen, the band gap of In_2O_3 is reduced from 3.5 eV to approximately 2.0 eV, thus electromagnetic radiation in the visible region can split water [21]. Zinc-doped gallium oxide is also an active photovoltaic device upon exposure to UV light [22]. Gallium has also been used to dope zinc oxide, producing transparent conductive films as an alternative to ITO thin films for optoelectronic and electronic devices such as flat panel displays [23], solar cells [24] and light-emitting diodes [25–28].

There are many techniques that have been reported to deposit thin films of gallium and indium oxide. These include chemical vapour deposition (CVD) (including aerosol assisted (AA) [29], low pressure (LP) [30] and atmospheric pressure (AP) CVD [31]); atomic layer deposition (ALD) [32,33]; sputtering [34,35]; sol–gel processes [36,37]; spray pyrolysis [38,39]; dip coating [40]; screen printing [41] and spin coating [42]. There are advantages and disadvantages for each of these methods: CVD processes tend to produce clean, uniform films but they are more complicated and expensive than the other methods which are simpler and cheaper, but typically produce non-uniform or non-stoichiometric films.

This review will detail gallium and indium complexes incorporating M–O bonds (M = Ga, In) with an emphasis on compounds employed as single-source precursors to gallium and indium oxide thin films. The presence of pre-formed M–O bonds can result in the formation of the metal oxide with fewer defects and at lower temperature. In addition, it is possible to deposit films using these precursors with simple apparatus and compounds that are easier to handle and characterize can be developed. However, there have been reports where MCl_3 and MMe_3 have been used as precursors to gallium and indium oxide thin films. In these cases, an additional oxygen source is needed which can include the following: O_2 [43], O_3 [44], air [45], H_2O [46], alcohols [31,47] and H_2O_2 [48] and generally high temperatures are required. Therefore, the demand to develop single-source precursors that decompose cleanly at lower temperatures, such that films can be grown on flexible substrates (e.g. plastics) with better optical and electronic properties is always increasing.

Synthetic chemists play a key role in designing and developing new single-source precursors. This review will highlight those compounds that have been used to form gallium and indium oxide films. The systems where an additional oxygen source is *required* to form metal oxide thin films, are not considered to be single-source routes (including ALD because the technique requires two sources to function correctly) and will not be covered in this review. Doped group 13 metal oxides (e.g. ITO) will also be excluded because there are a vast number of these types of materials, many of which have already been reviewed [17].

Discussion of group 13 metal oxide thin films will be divided into the following sections: single-source precursors to Ga_2O_3 thin films, single-source precursors to In_2O_3 thin films (incorporating mixed gallium indium oxide thin films) and recently published complexes incorporating M–O bonds that are potential precursors to gallium and indium oxide thin films, which updates the review published in 2006 describing gallium and indium alkoxides [49]. The following abbreviations will be used: acac (acetylacetonate); ALD (atomic layer deposition); bdk (β-diketonate); bzac (benzoylacetonate); CVD (chemical vapour deposition); dipp (2,6-diisopropylphenyl); DMAP (4-dimethylaminopyridine); EDX analysis (energy dispersive X-ray analysis); hfac (1,1,1,5,5,5-hexafluoroacetylacetonate); GED (gas-phase electron diffraction), GCMS (gas chromatography mass spectroscopy), ITO (tin-doped indium oxide); Mes (mesityl, 2,4,6-trimethylphenyl); RBS (Rutherford backscattering spectra); TCO (transparent conducting oxide), tfac (1,1,1-trifluoroacetylacetonate); thd (2,2,6,6-tetramethylheptane-3,5-dionate); SEM (scanning electron microscopy), XRD (X-ray diffraction), XPS (X-ray photoelectron spectroscopy), WDX (wavelength dispersive X-ray analysis).

2. Precursors to gallium oxide

Thin films of gallium oxide, Ga_2O_3, are commonly found in the monoclinic β form which has good chemical and thermal stability, as well as possessing interesting electrical properties. Although at room temperature it is an electrical insulator, it becomes semiconducting above 500 °C whilst exhibiting a response to reducing gases (e.g. CO, EtOH) and above 900 °C its electrical resistivity is sensitive to the presence of oxygen.

Although a recent (2006) review comprehensively surveyed the literature on gallium alkoxides, it did not focus on their application as precursors to thin films of gallium oxide [49]. In this section the synthesis and characterization of all single-source precursors to gallium oxide are described, as well as the reactor conditions used to deposit thin films of gallium oxide. However, because the previous review covered many of the featured precursors in depth, detailed discussion about their structural and physical properties has not been included. This section has been organised into 4 areas: single-source precursors comprising (i) monodentate alkoxides, (ii) donor-functionalized alkoxides, (iii) β-diketonates and (iv) other precursors.

2.1. Monodentate alkoxides

The structure of simple homoleptic gallium alkoxides of the type $[Ga(OR)_3]$ is dependent on the nature of R. For bulky R groups (e.g. R = ^{t}Bu), a dimeric structure with two bridging alkoxide groups and four terminal alkoxide groups arranged around two tetrahedral gallium centres is adopted. For slightly less bulky R groups (e.g. R = ^{i}Pr, ^{i}Bu) an analogous dimeric structure is in equilibrium with a tetrameric $[Ga\{Ga(OR)_4\}_3]$ structure (Fig. 1). These tetramers contain a central 6-coordinate octahedral gallium centre bound to three tetrahedral $Ga(OR)_4$ moieties through two bridging alkoxide groups per tetrahedral gallium centre. Two terminal alkoxide groups per tetrahedral gallium centre complete the coordination sphere. Gallium alkoxides with small R groups (e.g. R = Et) exclusively adopt the tetrameric structure.

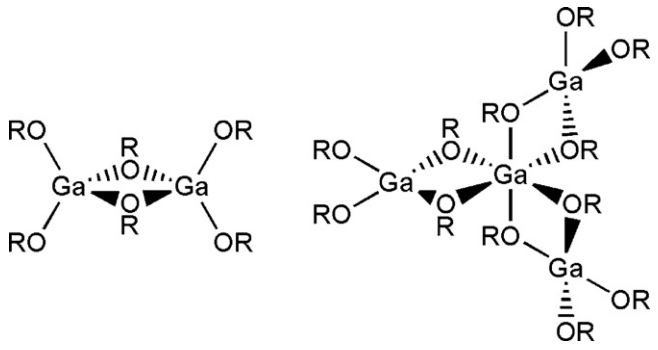

Fig. 1. Structure of $[Ga(OR)_3]_n$ as a dimer for large R groups ($n = 2$, R = ^{t}Bu) and a tetramer for small R groups ($n = 4$, R = Et).

The first synthesis of gallium alkoxides utilised the salt metathesis method, starting with $GaCl_3$ and 3 equiv. of NaOEt or NaO^{i}Pr, forming $[Ga(OEt)_3]$ and $[Ga(O^iPr)_3]$ respectively. With these two (and $[Ga(OPh)_3]$) in hand, alcohol/alkoxide exchange reactions considerably expanded the range of known heteroleptic alkoxides. However, a more general synthesis of gallium alkoxides was reported in 2001 where amide/alcohol exchange starting from $[Ga(NMe_2)_3]_2$ resulted in the synthesis of a vast range of gallium alkoxides (Scheme 1).

In keeping with 'classical' group 13 chemistry, monomeric gallium alkoxides can be isolated by breaking up the oligomeric structures through coordination of $[Ga(OR)_3]_n$ to a Lewis base. This was first observed in certain amide/alcohol exchange reactions where the use of bulky alcohols led to retention of one equivalent of $HNMe_2$. This resulted in the isolation of tetrahedral $[Ga(OR)_3(HNMe_2)]$ compounds (e.g. R = ^{t}Bu). Replacement of the dimethylamine moiety with DMAP (4-dimethylaminopyridine) was accomplished in some cases, with retention of the tetrahedral geometry at gallium (Scheme 2).

$[Ga(O^iPr)_3]_n$ is commercially available, making it a particularly attractive precursor. Kim et al. were the first group to take advantage of this, using it in a low pressure (LP)CVD chamber to deposit thin films of Ga_2O_3 [50]. The films were grown on a Si substrate heated to 400–800 °C at 1×10^{-7} Torr whilst the $[Ga(O^iPr)_3]_n$ was heated to 90–110 °C. The type and quality of film deposited was heavily dependent on the substrate temperature: below 500 °C the films were oxygen-deficient with a Ga:O ratio of 1:1. Above 700 °C the Ga:O ratio was much improved (1:1.6) but there was a significant amount of carbon contamination, mostly on the surface of the film. Between 500 and 600 °C, the films contained the correct Ga:O ratio and there was no trace of carbon contamination. All films grown were amorphous.

The organic byproducts from the CVD reaction were analysed by GCMS, revealing that propylene, 2-propanol and acetone were

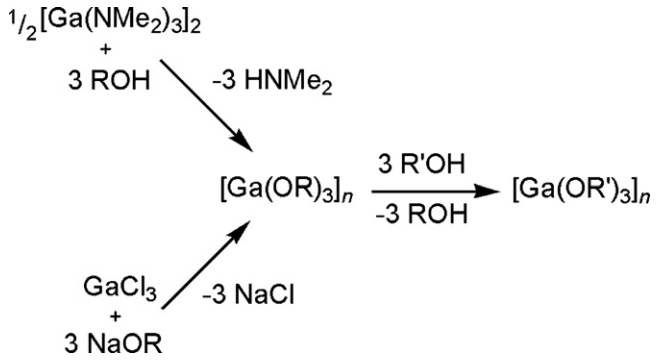

Scheme 1. Pathways to homoleptic gallium(III) alkoxides.

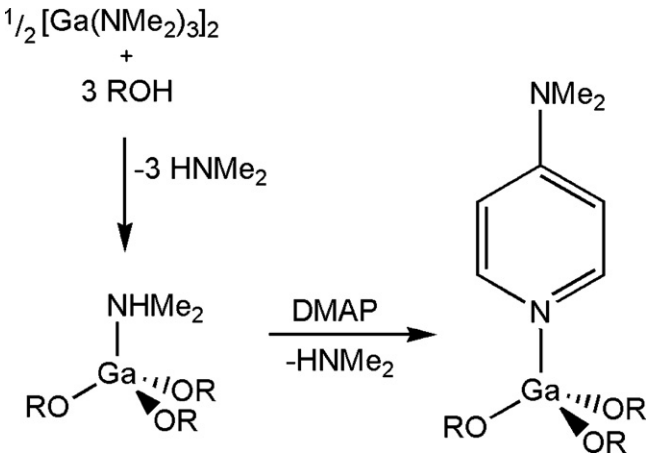

Scheme 2. Synthesis of Lewis base-stabilized gallium alkoxides.

the major byproducts. One proposed mechanism of decomposition involved β-hydrogen elimination of acetone followed by reductive elimination of 2-propanol, resulting in "Ga(O^{i}Pr)". This would then undergo γ-hydrogen elimination, forming propylene and "HGaO" which would further decompose, with loss of hydrogen, to Ga_2O_3 (Scheme 3).

The sol–gel method is another well-used technique for preparing thin films. Kokubun et al. have prepared Ga_2O_3 films by spin-coating sapphire substrates with a 2-methoxyethanol solution of $[Ga(O^iPr)_3]_n$ [51]. After spin coating, the substrates were heated at 90 °C to remove the solvent, then at 300 °C to remove organic contamination from the film. This was repeated 6 times before the films were annealed in air between 400 and 1200 °C. This time, the film quality was dependent on the annealing temperature: below 600 °C only amorphous films were deposited, but crystallinity was observed in films annealed above 600 °C. For temperatures greater than 900 °C some Al diffusion from the sapphire substrate to the Ga_2O_3 thin film was observed. The films demonstrated a response to UV light at wavelengths shorter than 270 nm; this response shifted to even shorter wavelengths as the annealing temperature increased, consistent with increasing amounts of Al contamination in the Ga_2O_3 film.

Li et al. have also used $[Ga(O^iPr)_3]_n$ to prepare films of Ga_2O_3 on sapphire substrates by the sol–gel method. A similar method to that described above was used, but these films were deliberately prepared with various dopants and will not be further discussed here [52]. Valet and Hoffman used the amide/alcohol metathesis method to synthesise a range of gallium alkoxides (Scheme 4) [53]. Starting from $[Ga(NMe_2)_3]_2$, reaction with 6 equiv. of secondary alcohol led to the isolation of tetrameric gallium alkoxides, which were in equilibrium with the dimeric structure. However, when tertiary alcohols were used, a mixture of the dimer and amine-stabilised monomer was isolated from the reaction. This mixture could be converted exclusively to the dimer by heating the mixture to drive off residual amine. Conversely, the amine-stabilised monomer could be exclusively formed by adding a large excess of dimethylamine to the dimeric alkoxide at room temperature.

The precursor chosen for LPCVD studies was compound **3**, mainly due to its low vapour pressure which was noted when sublimation of **3** was attempted. Films were grown on silicon, quartz and glass substrates at a range of temperatures (300–700 °C). Although these films were grown with O_2 as a co-precursor, a film was grown at 400 °C without O_2 and this proved to be of similar quality to the films grown with O_2. All films had the correct Ga:O ratio as judged from Rutherford backscattering spectra (RBS), although XPS data indicated that the films were slightly oxygen deficient (Ga:O ratio

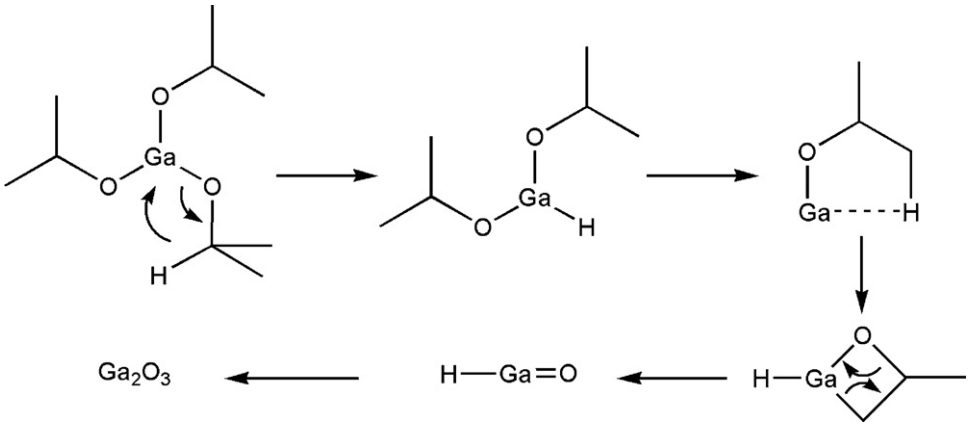

Scheme 3. Plausible decomposition of "[Ga(O^{i}Pr)$_3$]" under CVD conditions.

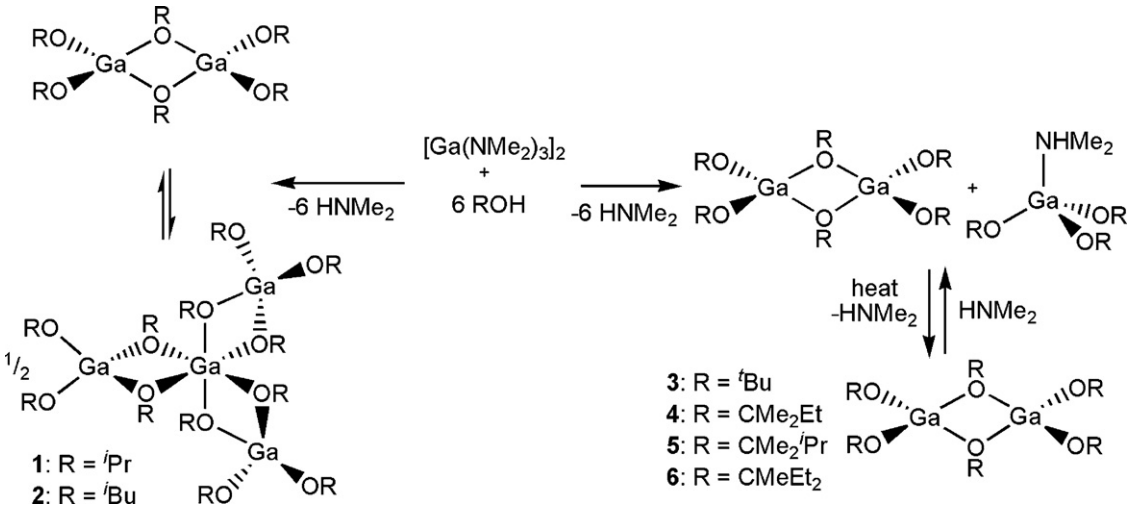

Scheme 4. Formation of dimeric and tetrameric gallium alkoxides.

1:1.1). All films grown proved to be amorphous, so annealing at 700 °C and 1000 °C for four hours was carried out. Annealing at the lower temperature did not furnish crystalline material, but after heating the films to 1000 °C, crystalline Ga_2O_3 was obtained: XRD data indicated that the monoclinic β form had been obtained.

Similar work had been published 2 years earlier, again by Hoffman and co-workers, this time utilising fluorinated alkoxides [54]. Again using $[Ga(NMe_2)_3]_2$ as a starting material, reaction with 6 equiv. of fluorinated alcohol (both secondary and tertiary) led exclusively to the formation of the amine-stabilised monomer (Scheme 5). In this case, heating the amine-stabilised monomer under vacuum did not lead to dissociation of the amine and formation of a dimer, indicating that the amine ligands are much more strongly bound to the fluorinated alkoxides.

Although compounds **7** and **9** in their pure state are solids, the crude reaction products **7–9** were all liquids which proved difficult to purify. Replacement of the dimethylamine ligand with DMAP led to the formation of solid compounds **10–12**, which were easily crystallised. Nonetheless, for LPCVD, liquids are generally favoured over solids due to their increased volatility and compound **7** was used to deposit thin films of Ga_2O_3 on glass. Amorphous films were obtained for substrate temperatures between 250 and 450 °C with thicker films being obtained at higher temperatures. As measured by RBS, the films contained negligible levels of contaminants (C, N, F) but the Ga:O ratio indicated the films were slightly gallium deficient.

A tetrameric gallium alkoxide was synthesised by Carmalt and co-workers from $GaMe_3$ and 4-methylbenzyl alcohol in a 4:9 ratio [55]. However, in this case a homoleptic gallium alkoxide was not isolated: instead, retention of one of the methyl groups was observed on each of the tetrahedral gallium centres (Scheme 6).

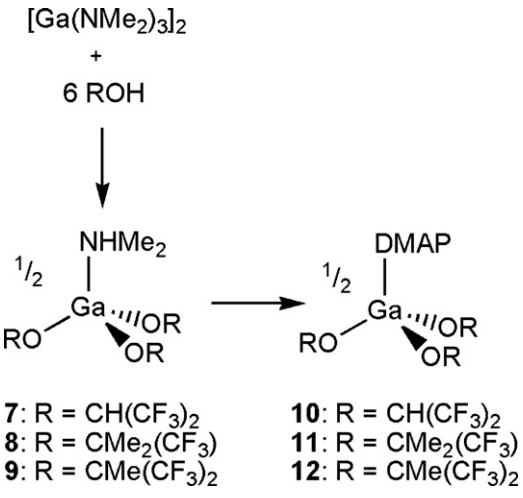

Scheme 5. Synthesis of fluorinated gallium alkoxides stabilised by Lewis bases.

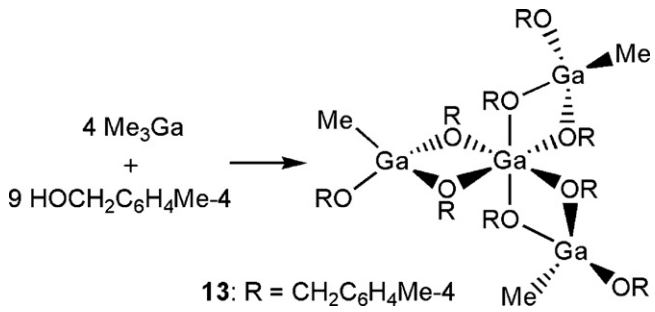

Scheme 6. Synthesis of tetrameric heteroleptic gallium alkoxides.

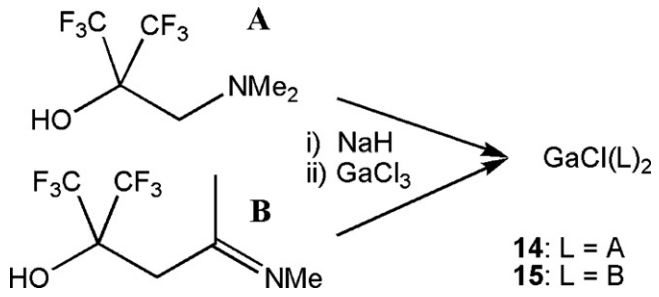

Scheme 7. First synthesis of gallium alkoxides using donor-functionalized alkoxides.

Compound **13** was used to deposit Ga_2O_3 thin films *via* LPCVD on glass at a substrate temperature of 600 °C. The Ga:O ratio could not be accurately determined by WDX owing to the thinness of the films; X-rays penetrated the films and breakthrough to the underlying glass substrate was observed. However, WDX did reveal the amount of carbon contamination was 1–2%. Interestingly, crystalline Ga_2O_3 was grown without the need for annealing: XRD of the films revealed the usual monoclinic β phase of Ga_2O_3 had been formed. Although this result is consistent with data reported by Kobukon et al., it is nevertheless unusual for crystalline films of Ga_2O_3 to be formed at temperatures as low as 600 °C [51]. The formation of crystalline films at such low temperatures may be the result of the 'core' of the precursor (i.e. not the 'terminal' substituents) containing the correct Ga:O ratio of 2:3.

2.2. Donor-functionalized alkoxides

Monomeric compounds are desirable for CVD owing to their higher volatility when compared to dimeric or tetrameric equivalents. Due to the electron-deficient nature of gallium, all of the alkoxides described above were dimeric/tetrameric, aside from when an additional Lewis base was used. Increasing the steric bulk at the gallium centre by use of bulky alkoxides (e.g. $OCPh_3$) does result in the formation of a monomeric compound, but this comes at a cost of vastly increasing the molecular weight of the precursor, hence reducing the volatility.

Another method of overcoming the oligomer problem is to use donor-functionalized alkoxides. These ligands were chosen for CVD, as they lead to precursors, which are less air/moisture sensitive and have increased solubility. These are alkoxides with one or more "arms", on the end of which is a Lewis base. The high moisture sensitivity of dialkylalkoxogallanes incorporating simple monofunctional alkoxides makes them difficult to use in solution-based CVD. However, the modified alkoxides with donor-functionalized ligands have an increased coordinative saturation at the metal centre and so provide stability. Furthermore, the donor-functionalized ligands eliminate the necessity of introducing an extra donor group to stabilize the electron deficient gallium alkoxide complex. The most popular donor-functionalized alkoxides are based on an alkyl backbone (C2 or C3) with simple Lewis bases (NMe_2, OMe), although more esoteric examples do exist in the literature.

Gallium compounds containing donor-functionalized alkoxides were first used as precursors to thin films of Ga_2O_3 in 2004 by Carmalt and co-workers [57] and Chi et al. [56].

Chi et al. used the salt metathesis method, reacting $GaCl_3$ with the sodium salts of fluorinated alkoxides to isolate bis(alkoxide) compounds of gallium (Scheme 7) [56]. Compounds **14** and **15** were both monomeric, 5-coordinate species, but they crystallised in different geometries. Whereas compound **15** is an almost ideal trigonal bipyramid in the solid state, compound **14** is exactly halfway between ideal trigonal bipyramidal and ideal square-based pyramidal geometry. This is probably due to a combination of steric factors (bulky CF_3 groups) and the different backbone size of the two ligands: the C2 backbone in compound **14** may not be long enough to allow formation of ideal trigonal bipyramidal geometry whilst minimising the steric interactions between neighbouring CF_3 groups.

An alternative method of single-source precursor synthesis is to react trialkylgallium reagents with donor-functionalized alcohols. In 2004 (and in subsequent years) this was utilised by Chi et al. (**16–18**) and Carmalt et al. (**19–28**) to form single-source precursors. Both mono(alkoxide) (below) and bis(alkoxide) (Section 4.2) compounds of gallium can be isolated although to date, no tris(alkoxide) complexes have yet been reported *via* this route (Scheme 8) [56–59].

Compounds **16–18** are monomeric, which is unusual for mono(alkoxide) gallium species which usually form oxygen-bridged dimers. It was thought the reason for this was the CF_3 groups: their steric bulk, coupled with the electron-withdrawing effect, reduced the ability of the alkoxide oxygen to form a bridge hence a monomer was isolated.

As is usual for mono(alkoxide) gallium complexes, compounds **19–26** were all isolated as oxygen-bridged dimers in the solid state, which was confirmed crystallographically (Figs. 2 and 3). However, gas-phase electron diffraction (GED) of compound **24** revealed that in the gas phase, it existed solely as a monomer (Fig. 4) [60]. The Ga–N bond length was significantly shorter in the monomer than in the dimer (2.332 Å and 2.471 Å respectively), consistent with a much more strongly bound ligand as would be expected from a less electron-rich complex. Therefore, although compound **24** adopts a dimeric structure in the solid state, it is monomeric in the gas phase. Monomers are expected to exhibit enhanced volatility in comparison to oligomeric complexes in which intermolecular solid-state

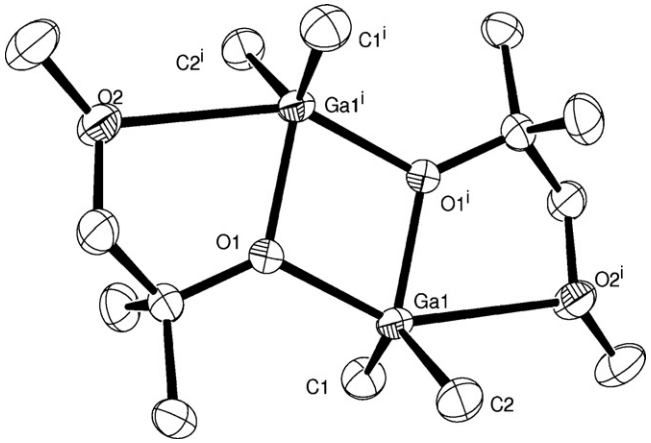

Fig. 2. ORTEP diagram showing gallium alkoxide compound **26** as a dimer with the Ga_2O_2 ring at the heart of the molecule. H atoms omitted for clarity.

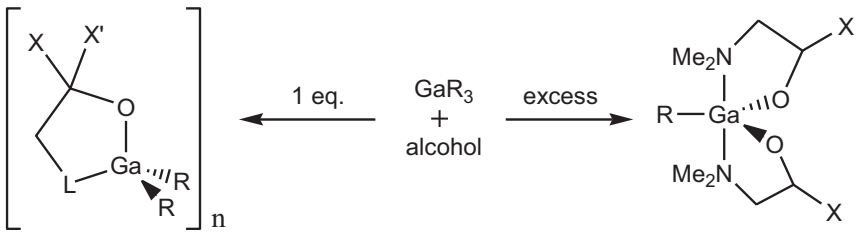

16: n = 1, R = Me, X = X' = CF_3, L = NHMe
17: n = 1, R = Me, X = X' = CF_3, L = NH^tBu
18: n = 1, R = Me, X = X' = CF_3, L = NMe_2
19: n = 2, R = Et, X = X' = H, L = NMe_2
20: n = 2, R = Et, X = CH_2NMe_2, X' = H, L = NMe_2
21: n = 2, R = Et, X = X' = H, L = OMe
22: n = 2, R = Et, X = Me, H' = H, L = NMe_2
23: n = 2, R = Et, X = X' = Me, L = OMe
24: n = 2, R = Me, X = X' = H, L = NMe_2
25: n = 2, R = Me, X = X' = Me, L = OMe
26: n = 2, R = Me, X = X' = H, L = OMe

27: R = Et, X = H
28: R = Et, X = Me

Scheme 8. Synthesis of non-fluorinated gallium alkoxides from trialkylgallium reagents.

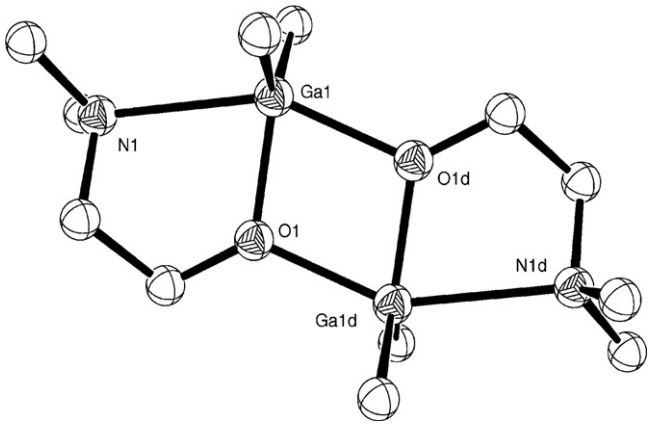

Fig. 3. ORTEP diagram showing the solid-phase structure of compound **24** as a dimer. H atoms omitted for clarity.

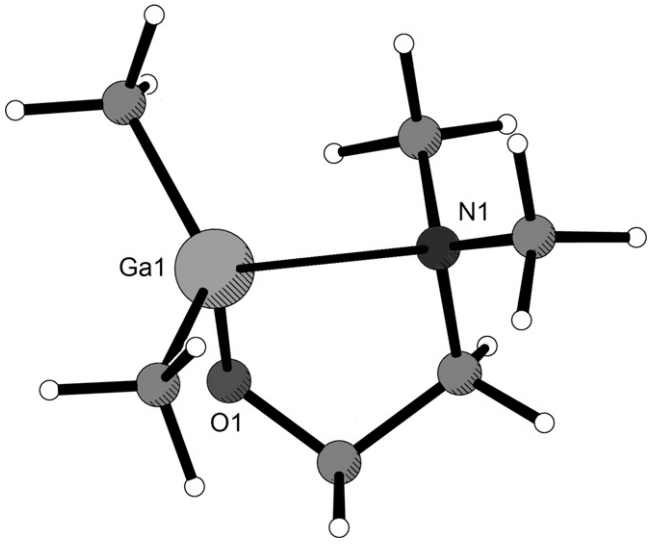

Fig. 4. Diagram showing the gas-phase structure of compound **24** as determined by GED.

interactions are likely to increase the enthalpy of vaporisation. In general, the structure adopted in the solid state may differ from that in the gas phase and so compounds that appear unsuitable for CVD may in fact be feasible precursors.

LPCVD of compounds **14** and **17** was carried out at 500–600 °C substrate temperature and pressure of 3 Torr (a small flow of O_2 was used as a carrier gas). Amorphous films were deposited on both quartz and silicon; annealing at 900 °C for 4 h induced crystallisation. XRD analysis of the annealed films indicated gallium oxide had been formed. XPS data showed a small amount of carbon contamination in the gallium oxide film, but other plausible contaminants such as N, F and Cl were not observed. The Ga:O ratio as measured by XPS indicated a slightly oxygen-deficient film had been formed, but RBS data showed Ga_2O_3 had been formed.

Compounds **19**, **20**, **22** and **23** were utilised as LPCVD precursors for Ga_2O_3 [57]. The LPCVD was carried out on quartz and glass substrates, heated to 600 °C. In each case the films grown were amorphous and no annealing was carried out. The films also contained a significant (*ca.* 10%) amount of carbon contamination, which was found by XPS. This also showed the Ga:O ratio was only 1:1.2, indicating an oxygen-deficient film had been formed. Whilst this is unsurprising considering the precursors were oxygen-deficient (Ga:O ratio of 1:1), XPS has not proven to be the most reliable method for analysing elemental ratios: many films thought to be oxygen-deficient when analysed by XPS turned out to contain the correct ratio when RBS was employed.

Since LPCVD resulted in oxygen-deficient films, compounds **19**, **20**, **22–26** were also used as aerosol-assisted CVD (AACVD) precursors [58,59]. All films were deposited on glass at a substrate temperature of 450 °C using toluene as solvent. For compounds **19**, **20**, **22** and **23**, the donor-functionalized alcohol was passed through the CVD reactor as a pre-treatment, but for compounds **24–26** this was not deemed necessary. For each run the precursor was generated *in situ* by reacting the free alcohol with GaR_3 (R = Et, Me), rather than using a pre-isolated compound. Each film grown was amorphous with low carbon incorporation (<0.1 at.%), located mainly at the surface, and no nitrogen contamination was observed. EDX of the films indicated the presence of oxygen, gallium and carbon but was an unreliable method of determining the Ga:O ratio due to breakthrough to the underlying glass substrate. WDX was more successful and a ratio very close to the expected 1:1.5 was observed

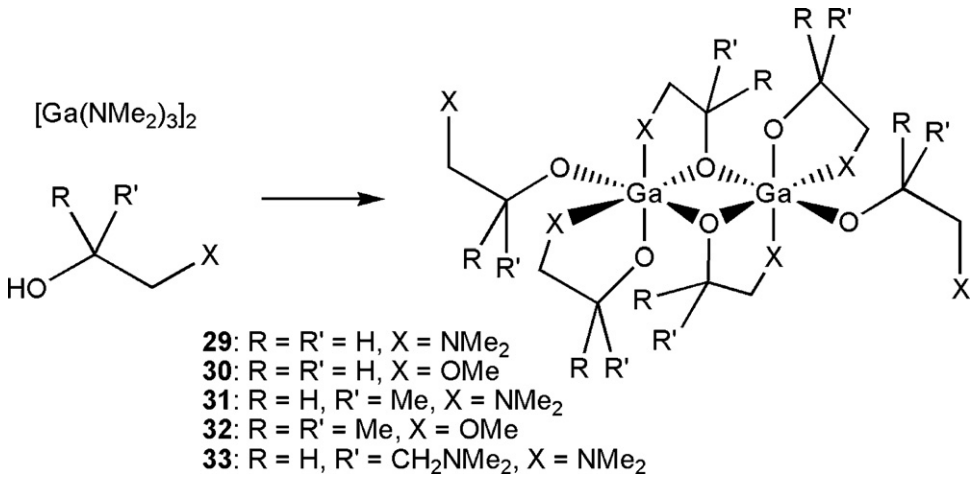

Scheme 9. Synthesis of homoleptic gallium alkoxides with donor-functionalized alkoxides.

in each case, albeit for exceptionally thin films this dropped to 1:1.3. The success of the *in situ* method indicates that synthesis, isolation and purification of the precursor is not always necessary in order to get successful Ga_2O_3 deposition, a factor which may prove to be an advantage for large-scale synthesis of Ga_2O_3 films.

Although the reaction of trialkylgallium compounds with alcohols yields both mono- and bis-substituted alkoxide complexes, replacement of all three alkyl groups with alkoxide groups was not possible. In order to isolate homoleptic gallium alkoxides with donor-functionalized arms, the amine metathesis route was utilised. Reacting dimeric $[Ga(NMe_2)_3]_2$ with 6 equiv. of donor-functionalized alcohol led to the formation of homoleptic gallium tris(alkoxide) complexes (Scheme 9) [3].

Somewhat surprisingly, the structure of compounds **29–33** was assigned as an oxygen-bridged dimer on the basis of mass spectrometry and IR spectroscopy (characteristic Ga_2O_2 ring stretches were observed at 557 and 538 cm^{-1}). ^1H NMR spectra were broad, with none of the expected coupling observed. This supported the idea of highly fluxional complexes containing dangling 'arms' associating and dissociating from the gallium centre on the NMR timescale: a formulation inconsistent with a monomeric complex where all 3 'arms' were strongly bound to gallium. Unfortunately, due to the oily nature of the products, structural characterization was not possible hence the exact coordination at the gallium centres remain unknown.

Compounds **29–33** were used as AACVD precursors, although they were not isolated prior to use in deposition reactions. In a continuation of the *in situ* methodology previously developed, $[Ga(NMe_2)_3]_2$ and the donor-functionalized alcohol (6 equiv.) were placed in an AACVD flask, allowed to react for 1 h and then passed into the CVD chamber. For each compound, deposition was carried out on glass with a substrate temperature of 550 °C. WDX analysis of the as-deposited films showed they were all oxygen-deficient, with a Ga:O ratio of 1:1.15. Subsequent annealing in air at 600 °C improved the Ga:O ratio to the expected 1:1.5 (as measured by WDX) but annealing at this temperature did not induce crystallisation of the films, despite appearing to have a snowflake-like morphology (Fig. 5). XPS data also indicated that Ga_2O_3 had been formed and that carbon contamination was limited to the surface of the film. No nitrogen contamination was observed.

Homoleptic gallium alkoxides were also prepared using the alcohol/alkoxide exchange method (Scheme 10) [36]. Starting from $[Ga(O^iPr)_3]$ and the free alcohol, compound **29** (above) with one "arm", as well as compounds **34** and **35**, with two and three "arms" respectively, were prepared in good yields. Although the solid state structures of **29** and **35** were not determined, it was possible to crystallise compound **34** and it was analysed by single crystal X-ray diffraction (Fig. 6).

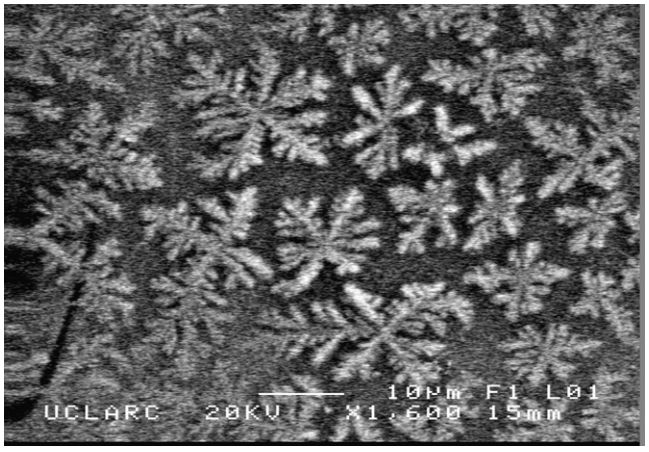

Fig. 5. SEM image of Ga_2O_3 grown by AACVD of compound **31**.

The overall structure of compound **34** is similar to that of the tetrameric gallium alkoxides (Section 2.1). There are two distinct gallium environments, but unlike the structure of the tetrameric gallium alkoxides, all gallium cations in the structure of **34** are octahedrally coordinated. The 'outer' gallium cations are bound to two ligands (thus the coordination sphere comprises four oxygen and two nitrogen atoms) with two alkoxide oxygen atoms per 'outer' gallium bridging to the central gallium, thus the coordination sphere of the central gallium is 6 alkoxide oxygen atoms.

Prior to their use in a spin-coating process to form gallium oxide, compounds **29–35** were hydrolysed in boiling water to determine the likely decomposition pathway. GaO(OH) was identified as the hydrolysis product, forming in its crystalline orthorhombic phase. Upon heating, it first become amorphous then started converting to Ga_2O_3 at 250 °C. At 500 °C, rhombohedral gallium oxide was observed by XRD: this then converted to the more usual monoclinic phase at 700 °C.

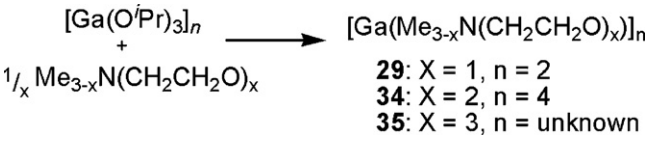

Scheme 10. Synthesis of gallium alkoxides with multiple 'arms' on the alkoxide.

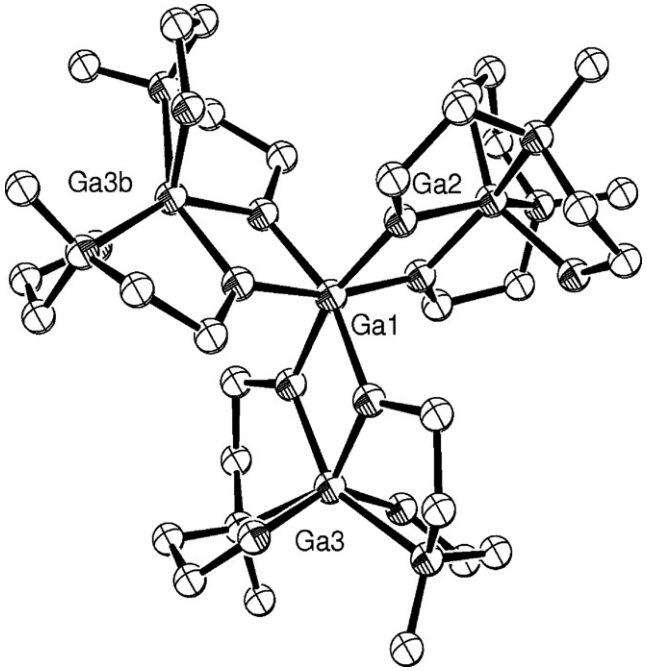

Fig. 6. ORTEP diagram of compound **34**. H atoms omitted for clarity.

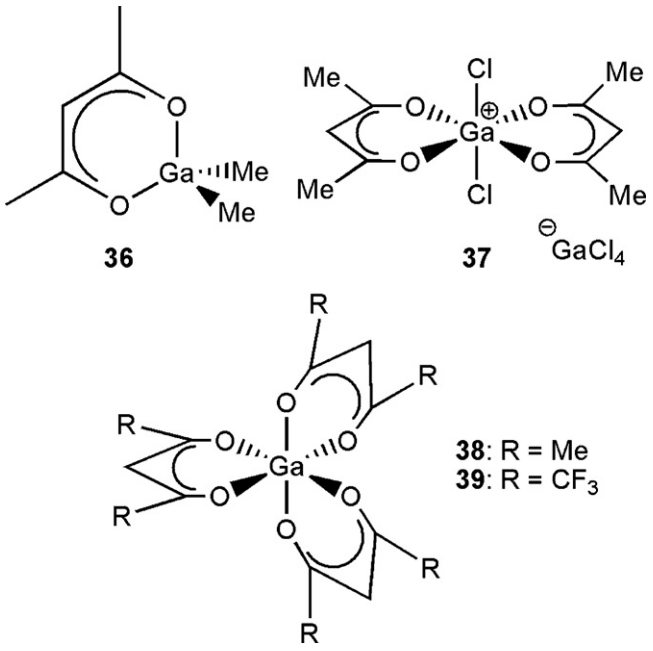

Fig. 7. Diagram of mono, bis and tris gallium β-diketonates.

These data were used to facilitate the spin-coating process. Compound **35** was hydrolysed and then dropped onto a glass or silicon substrate spinning at 1200–2000 rpm. After drying at 120 °C, the process was repeated a number of times until a sufficiently thick film had been formed. This was then annealed at 500 °C (glass substrate), affording an amorphous film which was consistent with Ga_2O_3, as identified by EDX. Although the film was adherent on glass substrates, it was poorly adherent on silicon which precluded annealing at temperatures which would enable crystalline Ga_2O_3 to form.

2.3. β-Diketonates

Another group of compounds which have found use as precursors to thin films of Ga_2O_3 are the homoleptic gallium tris(β-diketonates). These compounds, of general formula [Ga(bdk)$_3$] (bdk = β-diketonate) are monomeric, 6-coordinate octahedral compounds (Fig. 7). By far the most commonly used is [Ga(acac)$_3$] (acac = acetylacetonate), which is commercially available, but [Ga(hfac)$_3$] (hfac = 1,1,1,5,5,5-hexafluoroacetylacetonate) has also found use as a precursor. Mono(β-diketonates) such as [$GaMe_2$(acac)] (**36**) [61] are known compounds but have not been used as precursors to Ga_2O_3, whereas the only bis(β-diketonate) known (**37**) is an involatile ion pair, thus is unsuitable for CVD purposes [62].

Wu et al. were the first group to use [Ga(acac)$_3$] (**38**) as a precursor to thin films of gallium oxide [63]. The precursor was synthesised from [$Ga(NO_3)_3$] and Hacac before being dissolved in acetic acid. This solution was then used in a spray pyrolysis process with oxygen as a carrier gas, depositing gallium oxide on silicon and silica substrates heated to 450 °C. The as-deposited films were amorphous, consistent with a low temperature deposition, but upon annealing at 800 °C for 6 h crystalline Ga_2O_3 was formed in the β-phase. The band gap of Ga_2O_3 was calculated from transmission spectroscopy and is 4.79 eV, consistent with literature values.

Atomic Layer Epitaxy (ALE) was used by Nieminen et al. to deposit Ga_2O_3 from [Ga(acac)$_3$] [44]. However, as is common in ALE/ALD, a secondary source (in this instance water, oxygen or ozone) was also used in order to control deposition, thus making the process a dual-source method. Such processes fall outside the scope of this review and will not be further discussed.

Ortiz et al. used [Ga(acac)$_3$] as a 0.05 M solution in water/methanol (1:1 ratio, along with a small amount of acetic acid to ensure dissolution) in an ultrasonic spray pyrolysis process to deposit Ga_2O_3 on glass and quartz [64]. The substrate temperature varied from 300 to 500 °C inversely with the deposition time (15–30 min). As expected, the films were deposited as amorphous but annealing the quartz films at 900 °C resulted in the formation of crystalline β-phase monoclinic Ga_2O_3. RBS spectra of both the as-deposited and annealed films showed signals corresponding to silicon, in addition to the expected gallium and oxygen peaks. However, no carbon contamination was observed. Further analysis of the RBS data indicated that the films were composed of two 'layers': a surface layer almost entirely composed of Ga_2O_3 and a subsurface layer where gallium and oxygen had diffused into the silicon substrate. The formation of the extremely thermally stable SiO_2 was thought to be the driving force behind this process: IR spectra also contained an absorbance associated with the Si–O stretching vibration. Using optical transmission spectroscopy, the band gap was calculated as 4.94 eV (as-deposited films) and 4.99 eV (annealed films), consistent with literature values.

Deposition of Ga_2O_3 on silicon wafers was also carried out in a supercritical CO_2 ($scCO_2$) medium [65]. Parsons et al. used $scCO_2$ to dissolve [Ga(acac)$_3$] before heating the system to 160 °C, initiating decomposition of the precursor and film formation. The use of $scCO_2$ enabled much lower deposition temperatures to be utilised (some CVD processes run at >600 °C) but significant carbon contamination of the film of *ca.* 10 at.% was observed. Use of a co-oxidant (e.g. water) reduced the amount of contamination but did not completely eliminate it.

A fluorinated analogue of [Ga(acac)$_3$] can easily be synthesised by refluxing anhydrous $GaCl_3$ and 1,1,1,5,5,5-hexafluoroacetylacetone (Hhfac) in benzene. [Ga(hfac)$_3$] (**39**) is more volatile than [Ga(acac)$_3$] owing to the presence of fluorine in the molecule, which should assist low-pressure deposition techniques.

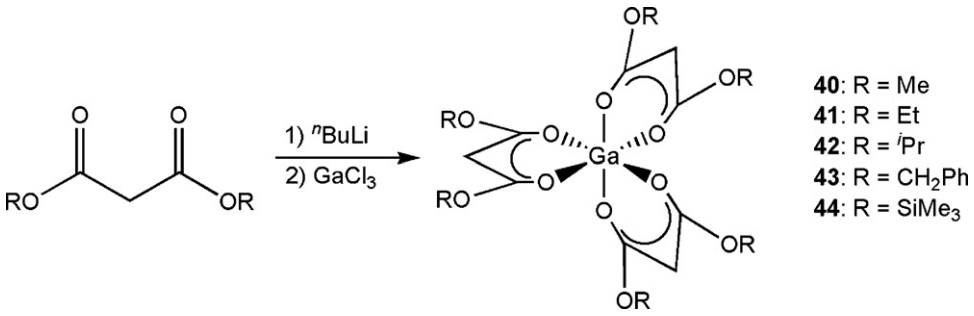

Scheme 11. Synthesis of gallium β-diketonates using malonic esters.

Porchia and co-workers used [Ga(hfac)$_3$] in an LPCVD process to form films of Ga_2O_3 [66]. An alumina substrate was heated to 450 °C and the precursor was passed over the substrate using a nitrogen carrier gas, with an overall system pressure of 26 mbar. The as-deposited films were black and amorphous, but annealing at 1100 °C resulted in the formation of a white, crystalline film of monoclinic Ga_2O_3. The Ga:O ratio was confirmed by XPS data, which also revealed very low amounts of carbon and fluorine impurities (<2%).

[Ga(hfac)$_3$] was also used as a precursor by Battiston et al., who deposited Ga_2O_3 films on both alumina and titania substrates [67]. Again an LPCVD process was used with an overall system pressure of 26 mbar, but this time the substrate was heated to 470 °C. The as-deposited films were black and amorphous but annealing at temperatures over 700 °C induced crystallisation. Films deposited on alumina exhibited some interdiffusion of the Al_2O_3 and Ga_2O_3 layers during the annealing process, probably due to the similarity in ionic radius between Al^{3+} and Ga^{3+}, but no interdiffusion was observed with the films grown on titania. XPS data of the as-deposited films indicated that stoichiometric Ga_2O_3 had been formed with low (<5%) carbon contamination.

Battiston et al. also found that a co-precursor of oxygen was necessary to minimise carbon contamination of the resulting films. Although films of Ga_2O_3 could be grown without a co-precursor, the resulting films were heavily contaminated with carbon (30%). No fluorine contamination was observed either: despite mass spectrometry data indicating that GaF_3 was a decomposition product of [Ga(hfac)$_3$], XPS data indicated no fluorine was present. One possible explanation was that GaF_3 was sufficiently volatile to be removed as a gas-phase byproduct under the reactor conditions.

Hellwig et al. synthesised a series of [Ga(bdk)$_3$] compounds (**40–44**) where the diketonate was the anion of a malonic diester (Scheme 11) [68]. The structures of these malonates was analogous to the diketonates, i.e. a 6-coordinate, octahedral gallium centre surrounded by 3 malonate anions, each binding through both carbonyl oxygen atoms to the gallium. Compound **41** was chosen for LPCVD owing to it having the lowest onset temperature of volatilisation of all 5 compounds. The presence of ester groups also provided additional cleavage sites, resulting in compound **41** having a lower decomposition temperature than 'classical' diketonates, e.g. [Ga(acac)$_3$]. Deposition occurred on a silicon substrate between 400 and 700 °C over a 60 min period. Nitrogen and oxygen were both used as carrier gases with the system pressure being maintained at 5 mbar throughout. All films were amorphous on deposition, even those deposited at 700 °C, but annealing at 1000 °C resulted in monoclinic Ga_2O_3 forming. EDX measurements indicated no carbon contamination of the film, but XPS data showed that a small amount of carbon contamination was present. This was removed upon erosion with Ar^+, indicating that the contamination was limited to the surface of the film only.

2.4. Other precursors

The three classes of precursor described above cover most of the single-source precursors to thin films of Ga_2O_3. However, some alternative single-source precursors have also been used, which are described in this section. Gallium nitrate, another commercially available gallium compound, has been used by the groups of both Hao and Cocivera [69] and Ohya et al. [70] to deposit Ga_2O_3.

Hao and Cocivera used a spray pyrolysis technique to deposit Ga_2O_3 on glass, quartz and aluminosilicate ceramic substrates. An aqueous solution of $Ga(NO_3)_3$ was atomised in an ultrasonic nebuliser and sprayed onto the substrate at 400 °C. Films were amorphous as-deposited, but annealing at 600 °C in a variety of atmospheres (air, N_2, Ar, 1:1 H_2:N_2) produced crystalline monoclinic films of Ga_2O_3. Increasing the annealing temperature to 900 °C improved the crystallinity of the films. The Ga:O ratio was not directly measured, but cathodoluminescence spectra of the as-deposited films showed a broad blue–green absorption. This absorption was explained as being the product of an oxygen-deficient film where recombination of an electron on a donor (formed by oxygen vacancies) with a hole on an acceptor (made up of either gallium vacancies or gallium–oxygen vacancy pairs). Further evidence came from analysis of the annealed films, where films annealed in a reducing or inert atmosphere showed a strong absorption but films annealed in an oxidising atmosphere exhibited a vastly reduced absorption, indicating the as-deposited films were oxygen-deficient.

Ohya et al. also used an aqueous gallium nitrate solution to form films of Ga_2O_3 on a glass substrate. Two techniques were used: dip-coating and spin coating, then the substrate was dried and heated to 700 °C. Crystalline Ga_2O_3 was obtained at this temperature and the films were transparent. Ga(O)OH was also used as a precursor; owing to its insolubility in water, it was dissolved in HCl and dip-coated onto a glass substrate. Decomposition to Ga_2O_3 was completed at 550 °C but the resulting transparent film was amorphous, hence the film was heated to 700 °C to induce crystallisation. Band gap measurements of the films resulted in agreement with literature values of 4.9 eV. The room temperature electrical resistivity of the film grown by spin coating was measured at $6 \times 10^7\ \Omega$ cm, confirming a high electrical resistance.

3. Precursors to indium oxide

Thin films of indium oxide, In_2O_3, are usually found in the cubic form. Unlike Ga_2O_3, at room temperature In_2O_3 is an electrical conductor and finds use as a TCO material, although it is usually doped with tin to enhance its electrical conductivity. However, this section is solely concerned with the synthesis and characterization of single-source precursors to undoped indium oxide, in addition to the conditions used to deposit thin films of indium oxide. Like the gallium oxide section, detailed discussion on the structural and physical properties of the precursors has not been included because

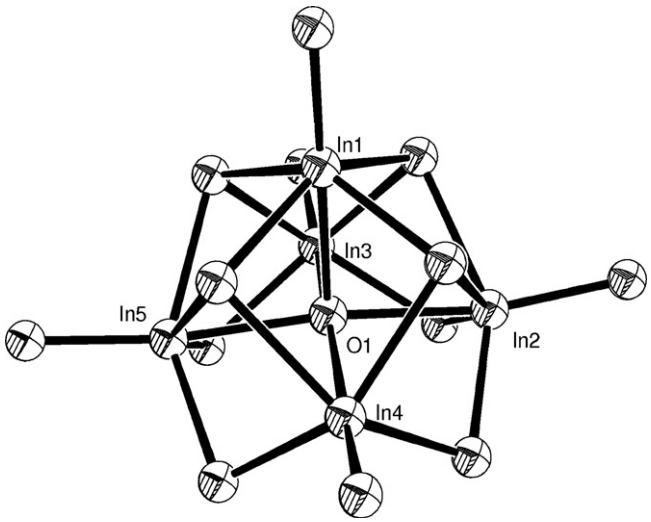

Fig. 8. ORTEP diagram of the indium cluster $[In_5(\mu_5\text{-}O)(\mu_3\text{-}O^iPr)_4(\mu_2\text{-}O^iPr)_4(O^iPr)_5]$. Hydrogen and carbon atoms omitted for clarity; the oxo anion (O1) is at the centre of the cluster.

it has previously been covered. Some details on film characterization have also been included.

Similarly to the gallium oxide section, this section has been divided into four areas: (i) simple monodentate indium alkoxides, (ii) donor-functionalized indium alkoxides, (iii) indium β-diketonates and (iv) other precursors. A short survey of single-source precursors to the mixed metal material indium gallium oxide has also been included.

3.1. Monodentate alkoxides

Compared to simple gallium alkoxides, the structure and reactivity of simple indium alkoxides is less well researched. "$[In(O^iPr)_3]$" was first reported in 1976 as a tetramer, supposedly analogous to $[Ga(O^iPr)_3]_4$ [71]. However, subsequent studies revealed it actually existed as an oxo-centred cluster of the type $[In_5(\mu_5\text{-}O)(\mu_3\text{-}O^iPr)_4(\mu_2\text{-}O^iPr)_4(O^iPr)_5]$ (Fig. 8), but the origin of the central oxide anion was unknown [72]. Similarly to the gallium compound $[Ga(O^iPr)_3]_4$, "$[In(O^iPr)_3]$" was used as a starting point to synthesise a range of simple indium alkoxides by alkoxide/alcohol exchange. However, the work carried out by Bradley et al. indicated that the alkoxides synthesised from "$[In(O^iPr)_3]_4$" may also be complex oxy-alkoxides, rather than a simple oligomer of $[In(OR)_3]$.

Nonetheless, Cantalini et al. used "$[In(O^iPr)_3]$" as a single-source precursor to thin films of In_2O_3 using the sol–gel technique [73]. The indium precursor was dissolved in ethanol, dropped onto a sapphire substrate and spun at 1000–3000 rpm for 20–60 s. After baking at 120 °C for 30 min, the films were annealed at 500 °C to induce crystallisation. XRD analysis of the annealed film revealed that cubic In_2O_3 had been formed, but XPS data indicated that the film was oxygen-deficient.

The use of amide/alcohol exchange as a technique for synthesising homoleptic indium alkoxides was restricted owing to the fact that simple homoleptic indium amide compounds, e.g. $[In(NMe_2)_3]_2$, were not readily available. However, Hoffman and co-workers used the bulky indium amides $[In\{N^tBu(SiMe_3)\}_3]$ and $[In(tmp)_3]$ (tmp = 2,2,6,6-tetramethylpyrrolidide) as starting materials for the synthesis of a range of homoleptic indium alkoxides by amide/alkoxide exchange [74]. This led to the formation of dimeric homoleptic indium alkoxide precursors from $[In\{N^tBu(SiMe_3)\}_3]$, rather than $[In(tmp)_3]$ on economic grounds (Scheme 12) [75].

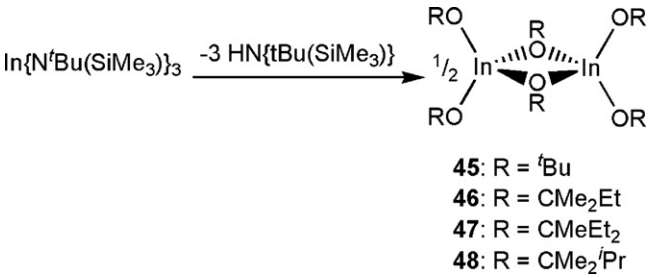

45: R = ^{t}Bu
46: R = CMe_2Et
47: R = $CMeEt_2$
48: R = $CMe_2{}^i$Pr

Scheme 12. Synthesis of dimeric In_2O_3 single-source precursors.

Compound **46** was chosen as a precursor owing to its low melting point (40–41 °C). Deposition of In_2O_3 on glass and silicon substrates was accomplished using an LPCVD process whereby the precursor was heated to 50 °C and the substrate was heated to temperatures between 300 and 500 °C. As is typical for the deposition of thin films of In_2O_3, the films deposited at all temperatures were crystalline as measured by XRD, with cubic In_2O_3 being observed in all cases. RBS spectra indicated that stoichiometric In_2O_3 had been formed and XPS data showed that no carbon contamination was present.

Another indium alkoxide was synthesised by Carmalt and co-workers who reacted $InMe_3$ with 4-methylbenzylalcohol in a 4:9 ratio (Scheme 13) [29]. Analogously to the gallium case (**13**), a tetrameric molecule was isolated with the 'core' of the molecule containing an M:O ratio of 4:6, ideal for In_2O_3. However, the biggest difference to compound **13** was found on the outer metal atoms; whereas only one methyl group was retained in the gallium compound, both methyl groups were retained for the indium precursor.

TGA of compound **49** indicated that decomposition to In_2O_3 was a facile process, but this was not borne out by CVD experiments. A black film was deposited on a glass substrate at 600 °C which was assigned to metallic indium on the basis of XRD analysis. Further investigations revealed that decomposition of compound **49** occurred before the melting point, which precluded transport of **49** into the CVD reaction chamber. No further CVD experiments were conducted on compound **49**.

3.2. Donor-functionalized alkoxides

Much like the situation for simple alkoxide compounds, there has been less research carried out into donor-functionalized alkoxide compounds of indium than gallium. Indeed, the paucity of suitable indium amide starting materials has resulted in $InMe_3$ being selected as the starting material of choice for the synthesis of donor-functionalized alkoxide CVD precursors. Chi et al. reacted a series of fluorinated donor-functionalized alcohols with $InMe_3$, affording a range of dimeric 5-coordinate indium complexes (Scheme 14).

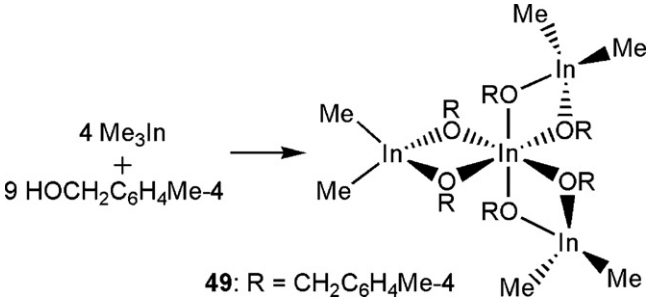

Scheme 13. Synthesis of a tetrameric indium oxide precursor.

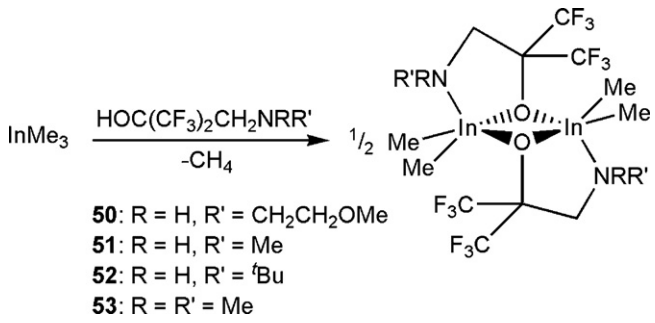

Scheme 14. Synthesis of fluorinated donor-functionalized indium complexes.

Even though compound **50** had two further 'arms' which were capable of coordination to the indium centre, single crystal X-ray analysis revealed that the 'arms' were dangling and did not coordinate. It also revealed that a 4-membered In_2O_2 ring was present at the core of the molecule, analogous to mono(donor-functionalized alkoxide) complexes of gallium with their Ga_2O_2 rings. Compound **51** was selected for LPCVD experiments: deposition occurred on quartz and silicon substrates at temperatures between 400 and 500 °C. The substrate was heated to 145 °C and the system pressure was maintained at 0.3 Torr. All films were crystalline as-deposited, with cubic In_2O_3 being the phase formed, although the degree of crystallinity increased with deposition temperature. XPS data indicated that a small amount of carbon was present as an impurity, but no fluorine could be detected. The In:O ratio, as measured by XPS, showed the films to be very oxygen-deficient but the more accurate RBS experiments indicated that stoichiometric In_2O_3 had been formed.

The use of non-fluorinated indium alkoxides as CVD precursors to indium oxide was initially developed by Carmalt and co-workers [29]. $InMe_3$ and a large excess of alcohol were reacted in toluene for 60 min, then the reaction mixture was passed straight into the CVD chamber using AACVD. Deposition occurred on glass at a temperature of 550 °C, affording brown films of cubic In_2O_3 as measured by XRD. WDX data indicated that most of the films were formed of stoichiometric In_2O_3, with the remainder being sufficiently thin that X-ray breakthrough to the underlying substrate was observed, adversely affecting the WDX analysis. XPS data did not indicate any carbon or nitrogen contamination of the films.

The formation of $[InMe_2(OR)]_2$ was assumed to take place *in situ* prior to the solution being passed into the CVD reactor. To confirm this, compounds **54–56** and **58** were synthesised and fully characterized (compounds **54–57** were used for CVD) by various spectroscopic techniques (Scheme 15).

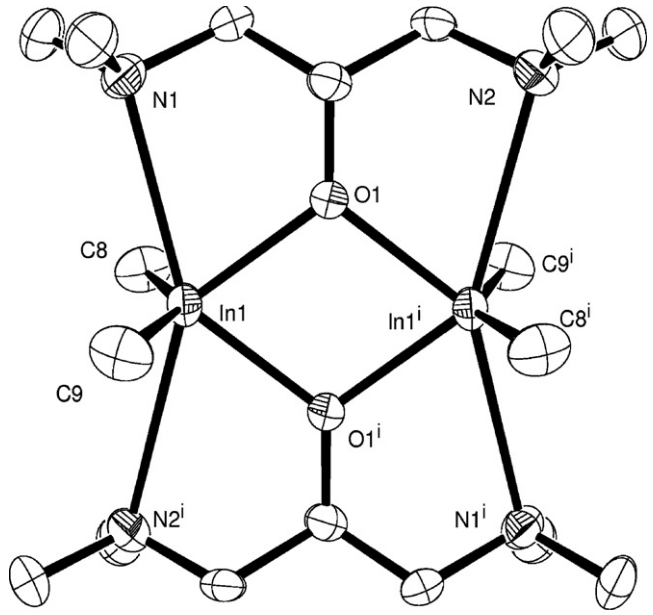

Fig. 9. ORTEP diagram of indium alkoxide compound **58** showing an unusual coordination mode whereby both "arms" bind to different metal centres. H atoms omitted for clarity.

Single crystal X-ray diffraction of the isolated compounds confirmed that in each case, a dimeric indium mono(alkoxide) had been formed (Fig. 9). Compound **59** was subsequently isolated and also fully characterized, but was not used for CVD purposes [59]. Interestingly, compound **58** where each ligand contained two 'arms' exhibited an unusual coordination mode whereby both 'arms' coordinated to the indium centres. This is in contrast to compound **50** which had a dangling 'arm', although this oddity can probably be put down to the geometry of the ligand: for compound **50** the alkoxide occurs at the end of the ligand whereas for compound **58**, the alkoxide occurs in the middle of the ligand. This enables the bridging alkoxide to coordinate to both indium centres in compound **58** because it has a Lewis base on either side, but for compound **50** only one side of the bridging alkoxide has a Lewis base therefore it cannot reach round and coordinate the second Lewis base to an indium centre.

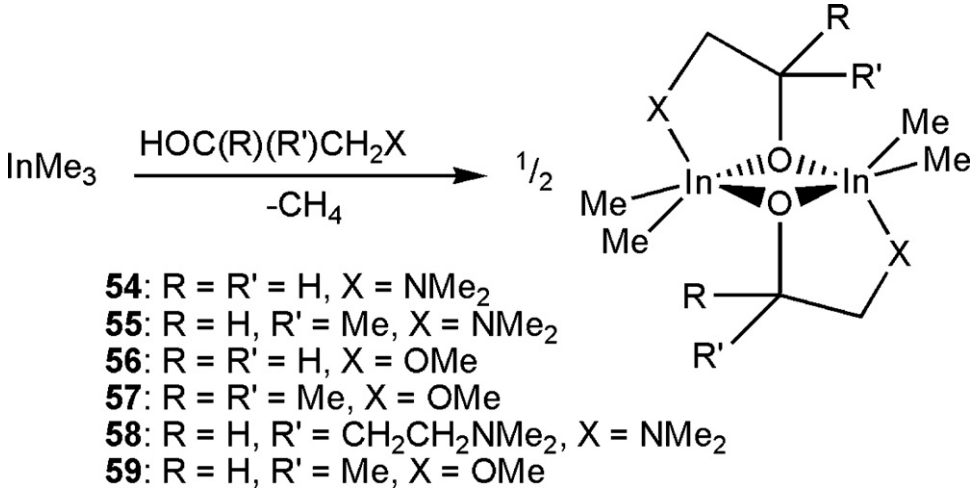

Scheme 15. Synthesis of non-fluorinated indium alkoxides with donor-functionalized ligands.

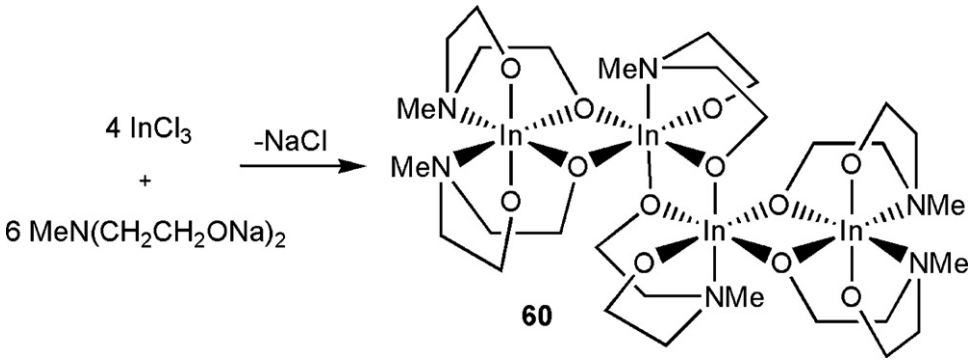

Scheme 16. Synthesis of dimeric indium-containing compound **60**.

These results are consistent with the case for donor-functionalized gallium alkoxides, where the room temperature reaction of $GaMe_3$ with an excess of alcohol only leads to the formation of mono(alkoxide) gallium compounds. Heating a mixture of $GaMe_3$ and excess donor-functionalized alkoxide to 110 °C results in the formation of a 1:1 mixture of mono- and bis(alkoxide) gallium compounds, and the same is true for indium [57]. However, under the reaction conditions inside the CVD flask, the *in situ* formation of indium mono(alkoxides) is the most likely outcome. To date, no bis(donor-functionalized alkoxide) indium compounds have been isolated and fully characterized.

The reaction of $InCl_3$ with 1.5 equiv. of freshly prepared $MeN(CH_2CH_2ONa)_2$ led to the formation of a dimeric indium tris(alkoxide) complex (Scheme 16) [36]. Compound **60** exists as a dimer with two $[InL_2]$ anions surrounding two central [InL] cations. One of the 'arms' of the ligand on the [InL] cation bridges to the other [InL] cation, forming the expected In_2O_2 ring at the centre of the molecule. The two $[InL_2]$ anions bridge twice to one [InL] cation, one 'arm' from each ligand forming the bridge. This results in the overall formation of an In_4-containing molecule which can best be described overall as existing in a zig–zag geometry. This is in contrast to the gallium analogue (Section 2.2) where the molecule formed a star-shape with one central Ga^{3+} cation and three $[GaL_2]$ anions.

The deposition of films of In_2O_3 from compound **60** was carried out in an analogous way to that of Ga_2O_3 films from compound **34**. Hydrolysis preceded spin-coating onto a glass or silicon substrate which was dried at 120 °C, before repeating the spin-coating several times to increase the thickness of the film. Unlike compound **34**, where [GaO(OH)] was identified as the hydrolysis product, for compound **60** $[In(OH)_3]$ was identified as the hydrolysis product. Annealing at 500–700 °C completed the process. The indium oxide film obtained was analysed by XRD, which confirmed the cubic phase of In_2O_3 had been formed. EDX analysis confirmed that stoichiometric In_2O_3 had been formed.

3.3. β-Diketonates

As is the case for gallium, homoleptic tris(β-diketonate) complexes of indium are an important class of single-source precursor (Fig. 10). The most commonly used precursor is $[In(acac)_3]$ (**61**), although $[In(thd)_3]$ (**62**) has also been used. Interestingly, the more volatile $[In(hfac)_3]$ has not been used as a precursor to thin films of pure In_2O_3, although it has been used as a precursor to doped indium oxide films. $[In(acac)_3]$ is commercially available whilst $[In(thd)_3]$ is easily prepared from hydrated $InCl_3$ and Hthd without the need for specialised equipment (i.e. inert-atmosphere techniques) [76]. All indium tris(β-diketonates) are 6-coordinate, octahedral species similar to their gallium congeners.

The first reported use of $[In(acac)_3]$ as a single-source precursor to thin films of In_2O_3 came in 1969, when Ryabova and Savitskaya used LPCVD to deposit on a variety of substrates [77]. The actual substrates used were not specified, but included a range of materials such as metals and semiconductors. The deposition temperature depended on the substrate used, with dielectric materials kept between 300 and 380 °C, semiconductors between 420 and 540 °C and metals between 450 and 650 °C. Interestingly, both amorphous and crystalline films were deposited with the crystallisation temperature varying according to substrate: crystallisation occurred at 360 °C on dielectric materials, but 490 °C and 500 °C on semiconductors and metals respectively. No further analysis was performed on the film.

Four years later, Korzo and Chernyaev also used $[In(acac)_3]$ to deposit indium oxide [78]. The indium precursor was melted, then the vapour carried into an activation chamber using a flow of argon. The $[In(acac)_3]$ was irradiated with high intensity UV light prior to passing into the deposition chamber, where it was deposited onto a variety of materials (e.g. silicon, quartz, sapphire, nickel, tantalum) between 270 °C and 520 °C. Annealing took place at the temperature at which deposition began upon the various substrates. Both amorphous and crystalline films were deposited, depending upon the deposition temperature.

Maruyama and Fukui used a range of indium carbonates and carboxylates (see Section 3.4) but also $[In(acac)_3]$ to deposit indium oxide films *via* an APCVD process [79]. The precursor was heated to 180 °C and carried into the deposition chamber by a flow of nitrogen gas. Deposition occurred on glass and quartz between 350 and 500 °C, with polycrystalline films being obtained at all temperatures. No further analysis was carried out on the In_2O_3 film.

$[In(acac)_3]$ was also used as a precursor in a spin-coating process by Tsuchiya et al. [80]. The precursor was dissolved in

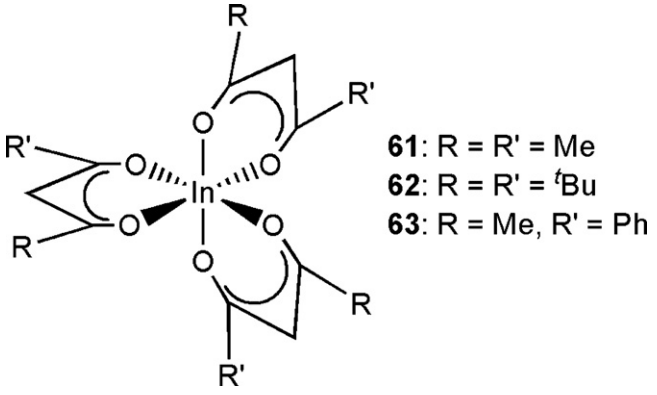

Fig. 10. Indium tris(β-diketonates) which have been used as single-source precursors.

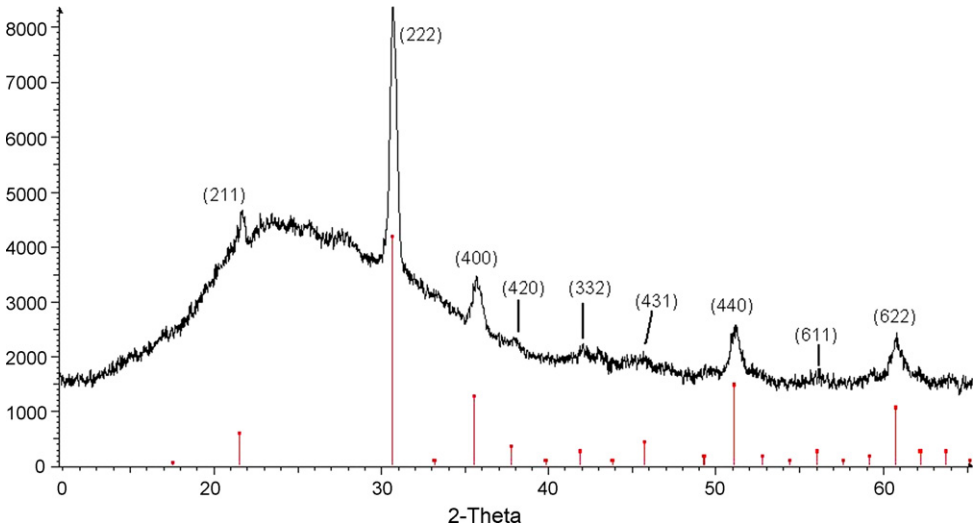

Fig. 11. Glancing angle XRD pattern of In_2O_3.

methanol/acetylacetone solution before spin-coating onto quartz or silicon substrates at 2000–4000 rpm. Drying in air at 150 °C for 10 min removed the solvents before photolysis with an ArF laser at room temperature led to the formation of indium oxide films. XRD analysis (e.g. Fig. 11) indicated that the expected cubic In_2O_3 had been formed.

Plasma-enhanced CVD (PECVD) of [In(thd)$_3$] led to the deposition of indium oxide thin films on aluminium at temperatures between 200 and 400 °C [81]. The reactor pipes had to be heated to 155 °C to prevent condensation of the precursor prior to it reaching the deposition chamber. Films grown below 350 °C contained a small amount of carbon (*ca.* 2 wt.%) but above this temperature, no carbon was detected. The film was characterized by elemental analysis, with stoichiometric In_2O_3 containing 82.7 wt.% In. Increasing the substrate temperature resulted in a slight drop in the indium content of the film to *ca.* 70 wt.% at 400 °C, but no carbon was observed implying a slightly oxygen-rich film had formed.

[In(thd)$_3$] was also used by Yoon and co-workers to deposit indium oxide on silicon at temperatures between 200–400 °C [82]. The precursor was dissolved in hexane before being vaporized and carried to the deposition chamber by a flow of argon. The films were all deposited as crystalline films, with the cubic In_2O_3 phase being identified from XRD experiments. XPS data indicated the composition of the film was consistent with In_2O_3, with no metallic indium observed, although a small amount of [In(OH)$_x$] was present at the surface of the film. A small amount of carbon contamination was also observed.

A slightly different precursor, [In(mbm)$_3$] (mbm = monobenzoylacetonate, **63**, Fig. 10) was synthesised from the aqueous reaction of [In(NO$_3$)$_3$] and Hmbm with ammonia [83]. After isolation as a white powder, it was dissolved in CH_2Cl_2 then dropped onto a silicon substrate spinning at 1500 rpm, before photolysis in air with a 254 nm UV lamp photolytically decomposed the precursor to indium oxide. Acetone was used to wash any remaining organic byproducts off the surface of the film. The as-deposited film was analysed by Auger electron spectroscopy, indicating that stoichiometric In_2O_3 had been formed albeit with a significant amount (*ca.* 20%) of carbon contamination. This was mostly localized at the surface, however, and argon sputtering for 5 min reduced the carbon contamination below 5%. Annealing of the as-deposited film at 900 °C for 2 h allowed XRD analysis to take place, confirming the cubic phase of In_2O_3 had been formed.

In contrast to the case for gallium, where mono(β-diketonate) compounds had not been used as a CVD precursor, one mono(β-diketonate) complex of indium has been synthesised and used to deposit indium oxide [30]. [$InMe_2$(OMe)] was reacted with Hacac in cold toluene, forming a mono(β-diketonate) compound of indium [$InMe_2$(acac)]$_2$ (**64**, Scheme 17).

Compound **64** is a dimeric 5-coordinate indium mono(β-diketonate) which is half-way between trigonal bipyramidal and square-based pyramidal geometry. The central In_2O_2 ring is formed through one of the oxygen atoms on the ligand, resulting in the diketonate twisting away from the methyl groups on the metal centre. This results in a significant difference in the In–O bond lengths [2.253(2) Å *vs.* 2.194(2) Å] but the In–C bond lengths are identical. The In–O bond length of the 'bridge' is noticeably longer at 2.606(3) Å, indicating a weak interaction holding the dimer together.

TGA analysis of compound **64** indicated sublimation occurred between 130 and 210 °C. Deposition on glass, silicon and GaAs substrates was carried out using LPCVD, with substrate temperatures of 350–450 °C. The precursor was maintained at a temperature of 150 °C throughout. All films were crystalline as-deposited according to XRD; the cubic phase of In_2O_3 was formed throughout. EDX analysis indicated that indium was present, although the In:O ratio could not be determined.

A modification of the β-diketonate ligand architecture is to form a β-ketoiminate ligand, with NR (R = alkyl, aryl) replacing one of the oxygen atoms. This is half-way between a β-diketonate and the 'NacNac' class of ligand which has many applications in synthetic chemistry, not least the ability to stabilise metals in unusually low oxidation states or coordination geometries [84,85]. Chi and co-workers used a β-ketoiminate as a ligand, synthesised

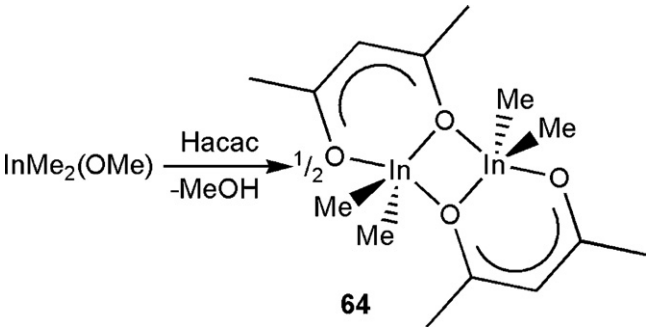

Scheme 17. Synthesis of indium mono(β-diketonate) CVD precursor **64**.

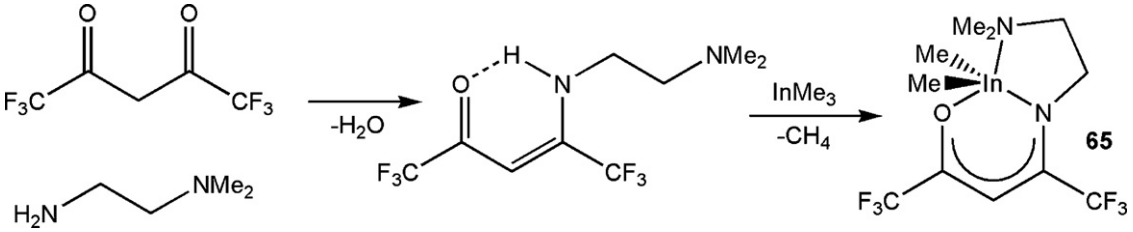

Scheme 18. Synthesis of indium (β-ketoiminate) CVD precursor.

by condensation of N,N-dimethylethylene diamine with Hhfac, to form the donor-functionalized (β-ketoiminate) CVD precursor **65** (Scheme 18) [86].

After isolation of the β-ketoimine ligand, reaction with $InMe_3$ and sublimation of the crude product afforded crystals of compound **65**. It exists as a monomeric 5-coordinate indium compound, best described as highly distorted trigonal bipyramidal. The In–O bond length of 2.251(3) Å is consistent with the long In–O bond length in compound **64** and the In–C bond lengths are identical. There is a marked difference between the two In–N bond lengths, with the In–N dative bond at 2.428(2) Å longer than the ketoiminate In–N bond of 2.321(2) Å.

TGA of **65** resulted in almost complete sublimation of the precursor, a good indicator of its stability at high temperatures. Compound **65** was heated to 80 °C to aid volatilisation in the LPCVD process and a small flow of O_2 as carrier gas was also used to transport the vapour into the deposition chamber. This resulted in crystalline films of cubic indium oxide being deposited on silicon and quartz at temperatures between 400 and 500 °C. XPS indicated that no carbon, nitrogen or fluorine impurities were present and RBS analysis indicated that stoichiometric In_2O_3 had been formed.

3.4. Other precursors

Unlike the case for gallium, several other indium compounds have been used as single-source precursors for thin film deposition. Indium nitrate is a commercially available compound which was first used as a single-source precursor in a sol–gel process by Tahar et al. [87]. Commercial indium nitrate was reacted with ammonia before washing with water and nitric acid to form the stable sol. It was thought from molecular weight measurements that the indium-containing species was $[In_2(OH)_5(NO_3)]$. Dip-coating onto glass substrates followed by drying in air at 110 °C and annealing at 300–600 °C formed a thin film of indium oxide, and the dip coating process was repeated several times to increase the film thickness. XRD analysis of the dried film pre-annealing indicated that $[In(OH)_3]$ had been deposited, which became amorphous upon annealing at 200 °C. Heating above 300 °C resulted in the formation of cubic indium oxide.

The sol–gel process was also used by Gurlo et al. to form indium oxide thin films [88]. Using the same method described above to form a sol, coating onto sapphire substrate followed by air-drying at room temperature and annealing at 700 °C afforded thin films of indium oxide. XRD characterization was not carried out, but XPS analysis was, indicating indium oxide had been formed. However, electron spin resonance (ESR) spectroscopy indicated that a small amount of paramagnetic In(II) ions were present in the lattice, indicating oxygen-deficient films had been formed. Heating the film in a reducing atmosphere (H_2 gas) increased the amount of In(II) found in the structure.

Indium nitrate, as a solution in 2-methoxyethanol, was used in an ultrasonic spray pyrolysis procedure by Lee and Park, depositing indium oxide onto bare glass at temperatures between 450 and 500 °C [89]. Deposition times varied between 30 and 120 min, with thicker films being formed at longer deposition times. Unusually, the films deposited at 450 °C were amorphous, with crystalline material being formed at temperatures above 500 °C. XRD analysis of the crystalline material indicated cubic In_2O_3 had been formed.

Indium hydroxide is another commercially available compound which has been used to form indium oxide. In 1998, Chung et al. made $[In(OH)_3]$ by hydrolysis of $InCl_3$ in the presence of ammonia, then used the spin-coating method to form a film of $[In(OH)_3]$ on alumina [90]. The film was dried at 110 °C then annealed at 400 °C for 1 h. This was repeated several times before a final annealing step at 600 °C afforded an indium oxide film. XRD analysis indicated the usual cubic phase of indium oxide had formed, but no further film characterization was carried out. Subsequent deposition of thin films on silica was also carried out using the same methodology, again forming cubic indium oxide as measured by XRD [91,92].

Tamaki et al. also used an $[In(OH)_3]$ sol, prepared as above, to deposit indium oxide [93]. The sol was dropped onto a silica substrate patterned with gold electrodes, dried and annealed at 600 °C. No film characterization was carried out, but SEM images showed grains of a material, probably indium oxide, on films annealed at 600 °C. Increasing the annealing temperature to 700 °C resulted in agglomeration of the grains into cubes and subsequently spheres at 850 °C.

A series of indium carboxylates has also found application for the deposition of undoped thin films of indium oxide. Indium acetate, $[In(OAc)_3]$, was first used in 2008 as a solution in 2-propanol, stabilised with lactic acid [94]. Six cycles of dip-coating onto a glass substrate, followed by annealing between 200 and 500 °C resulted in the formation of indium oxide films. The film annealed at 200 °C was amorphous, but all films annealed at higher temperatures were formed of cubic indium oxide as measured by XRD. In some cases, a second annealing of the films was carried out which exhibited improved electrical conductivity compared to films which had not undergone a second annealing step [95].

Indium acetate hydroxide, $[In(OAc)_2(OH)]$, was used by Maruyama and Tabata to deposit indium oxide on glass, heated to 300 °C [96]. The indium acetate hydroxide was not heated to a specific temperature, rather it was placed as close as possible to the glass substrate inside the deposition chamber, owing to its extremely rapid decomposition. XRD of the as-deposited films indicated they were composed of crystalline cubic indium oxide, but no further film characterization was carried out.

Indium tris(2-ethylhexanoate) is a slightly incongruous, yet commercially available, precursor to thin films of undoped indium oxide. It was first used in 1990 by Maruyama and Fukui to deposit indium oxide on a glass substrate heated between 350 and 400 °C [19]. The precursor was heated to 280 °C under a flow of nitrogen gas, which transported it onto the heated substrate. The as-deposited films were crystalline, with XRD analysis indicating that cubic indium oxide had formed [97].

Ching and Hill later used the same precursor to deposit indium oxide onto silicon substrates [98]. A thin film of the precursor on silicon was formed by the spin-coating method, before pho-

tolysis with a 254 nm UV light source resulted in decomposition of the precursor and formation of an indium oxide film. Auger spectroscopy of the as-decomposed film revealed the surface was heavy with carbon-containing contaminants, but after sputtering the stoichiometry of the film was confirmed as In_2O_3. The film was amorphous, however. Mass spectrometric analysis of the organic byproducts indicated the presence of CO_2, 2-heptene (and related isomers) and heptane, expected decomposition products from a C7-alkyl chain in the precursor.

Indium tris(2-ethylhexanoate) was also used as a precursor in a spin-coating process by Tsuchiya et al. [80]. The precursor was dissolved in toluene before spin-coating onto quartz or silicon substrates at 2000–4000 rpm. Drying in air at 200 °C for 10 min removed the solvent prior to room temperature photolysis with an ArF laser, leading to the formation of indium oxide films. XRD analysis indicated that cubic In_2O_3 had been formed, in contrast to the results obtained by Ching and Hill where room temperature photolysis with a UV light source did not result in the formation of crystalline films. No further film analysis was carried out.

Shigeno et al. used a slightly modified version of indium tris(2-ethylhexanoate) by replacing one of the carboxylate groups with a hydroxyl anion [40]. Thus, indium bis(2-ethylhexanoate)(hydroxide) was dissolved in an ethanol/xylene solution, dip-coated onto glass and heated to a temperature between 100 and 500 °C by an IR lamp. The film heated to 100 °C was crystalline, but decomposition had not taken place and the precursor was the only compound present. The film heated to 500 °C was consistent with cubic indium oxide, whereas the films heated to intermediate temperatures were consistent with neither, rather being tentatively identified as decomposition intermediates between the precursor and indium oxide.

3.5. Indium gallium oxide

Indium gallium oxide is a mixed metal oxide which also falls into the TCO class of materials. It was first characterized in 1994 as the stoichiometric mixed metal oxide, namely $InGaO_3$. XRD measurements showed it to be based on the monoclinic Ga_2O_3 lattice with indium cations replacing half of the gallium cations [15].

Initial reports of the material were all based around its synthesis by sputtering of Ga_2O_3 and In_2O_3 targets, a process outside the scope of this review. Nonetheless, a detailed study of the lattice structure with variation of the In:Ga ratio was carried out by Edwards et al. using XRD analysis of films grown using sputtering [99]. It was found that for gallium indium oxide of formula $In_{2x}Ga_{2-2x}O_3$, the value of x determined the lattice structure of the mixed metal oxide. For $x \leq 0.43$, the lattice structure was based on monoclinic Ga_2O_3 with replacement of some gallium cations by indium cations. For $x \geq 0.95$, the lattice structure was based on cubic In_2O_3 with substitution of some indium cations by gallium cations. For $0.43 < x < 0.95$, phase segregation occurs with the formation of monoclinic Ga_2O_3 and a separate mixed metal oxide phase based on the In_2O_3 cubic lattice. This is not wholly consistent with the work by Cava et al. who only observed a monoclinic Ga_2O_3-type lattice for $x = 0.50$ [15].

Whilst well-defined single-source precursors to gallium indium oxide are unknown, the material has been made using a combination of single-source precursors for gallium oxide and indium oxide. Marks and co-workers used a mixture of $[Ga(thd)_3]$ and $[In(thd)_3]$ in a dual-source LPCVD process to form films of $In_xGa_{2-x}O_3$, where $0.9 \leq x \leq 2.0$ [100]. The precursors were kept separate throughout the CVD process with $[Ga(thd)_3]$ being heated between 86 and 90 °C under a 5–20 sccm argon gas flow and $[In(thd)_3]$ heated between 98 and 104 °C under a 50–80 sccm argon gas flow. Deposition occurred on quartz and zirconia at temperatures between 400 and 650 °C and the reactor pressure was maintained at 4.7 mbar. For deposition on quartz, a substrate temperature of 500 °C was ideal, with lower temperatures increasing the amount of carbon contamination in the film.

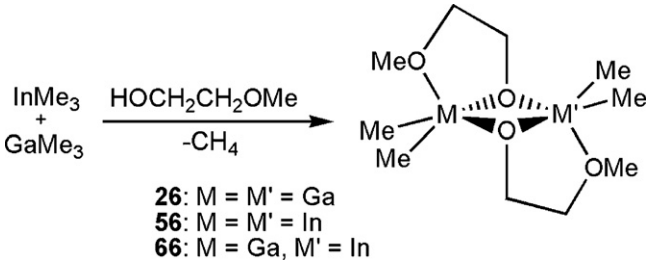

Scheme 19. Synthesis of bimetallic precursors to indium gallium oxide.

XRD analysis of the films grown for film compositions ranging from pure In_2O_3 to $In_{0.9}Ga_{1.1}O_3$ indicated that they were based on a cubic In_2O_3 lattice with substitution of some indium atoms for gallium atoms. No phase separation was detected, contrasting with the work of Edwards et al. who detected both a cubic In_2O_3-type lattice and a monoclinic Ga_2O_3-type lattice for film compositions of $In_{0.9}Ga_{1.1}O_3$. However, for more gallium-rich films, phase separation was detected. For all film compositions, annealing the as-deposited film under a reducing atmosphere at 400–420 °C increased the electrical conductivity. However, the film composition with the highest electrical conductivity was $In_{1.88}Ga_{0.12}O_3$.

Thin films of indium gallium oxide were also grown utilising an *in situ* CVD method [101]. A mixture of $InMe_3$, $GaMe_3$ and excess 2-methoxyethanol in toluene were allowed to react for 10 min before being passed into an AACVD reactor. The identity of the actual precursor is unknown, but based on previous work with MMe_3 and donor-functionalized alkoxides (M = Ga, In), it is thought a bimetallic oxygen-bridged species is formed with each metal retaining two methyl groups (Scheme 19).

No compounds were isolated and characterized from the reaction, but it is likely that a statistical mixture of products has formed. The mixed-metal precursor **66** should be the dominant product of the reaction, with significant amounts of compounds **26** and **56** also present.

Films were grown on glass substrates heated between 350–450 °C. It was found that the In:Ga ratio increased as the substrate temperature increased, with film composition $In_{0.77}Ga_{1.23}O_{2.44}$ observed at 350 °C and $In_{1.4}Ga_{0.6}O_{3.1}$ observed at 450 °C. The In:Ga ratio was determined by EDX, WDX and XPS analysis, with XPS data confirming that only one environment for each metal was present in the film. The as-deposited films were amorphous, but annealing at 1000 °C for 16 h resulted in the formation of crystalline films. XRD of the annealed film initially deposited at 450 °C revealed that the material was based on a cubic In_2O_3 lattice with substitution of some indium cations for gallium – no peaks corresponding to a monoclinic Ga_2O_3-type lattice were observed. Concomitant with this was a contraction in the lattice parameter from 10.12 Å (pure In_2O_3) to 9.84 Å, consistent with replacing larger indium cations with smaller gallium cations.

4. Potential precursors

There are a range of gallium and indium complexes containing preformed M–O bonds which have been reported, but have not been used to deposit M_2O_3 films (M = Ga, In). Comprehensive reviews of gallium and indium alkoxides, aryloxides and sesquialkoxides have been published [49,102], but the post-2006 literature has not been reviewed.

Herein we review gallium and indium compounds incorporating oxygen-based ligands that have been published since 2006,

Table 1
Selected Bond Lengths and Angles for M–O (M = Ga, In) compounds.

No.	Compound	Framework	M–O bond length (Å)	O–M–O bond angle (°)	M–O–M bond angle (°)	Reference
69	$[GaMe_2(OCH_2CH_2CH_2NHMe)]$	$GaONR_2$ core, tetrahedral	1.875(6)			[103]
72	$[Ga^tBu_2(OCH_2CH_2CH_2NHMe)]$	$GaONR_2$ core, tetrahedral	1.870(2)			[103]
73	$[Ga^tBu_2(OCH_2CH_2NH^tBu)]_2$	Ga_2O_2 ring, planar	1.955(2) 1.956(2)	76.9(2)	103.7(2)	[103]
74	$[Ga^tBu_2(OCH_2CH_2CH_2NH^tBu)]_2$	Ga_2O_2 ring, slightly folded	1.951(2) 1.957(2) 1.967(2) 1.951(2)	77.1(1) 76.9(2)	102.7(1) 103.0(1)	[103]
75	$[Ga(OC(CH_3)_2CH_2OMe)Cl_2]_2$	Ga_2O_2 ring, planar	1.9753(17) 1.886(2)	77.98(7) 76.30(9)	103.7(1) 103.7(1)	[104]
79	$[Ga\{O_2C(3,5\text{-}C_6H_3Me_2)\}\{CH(SiMe_3)_2\}]_2$	Ga_2O_2R core, tetrahedral	2.004(6) 2.004(6) 2.027(6) 2.010(6)	93.7(3) 93.1(3)		[105]
81	$[Ga_2\{CH(SiMe_3)_2\}_2(bzac)_2]$	Ga_2O_2R core, tetrahedral	1.959(3) 1.948(3)	91.1(1)		[107]
83	$[GaCl(acac)]_2$	Ga_2O_2Cl core, tetrahedral	1.888(6) 1.889(6)	95.3(3)		[108]
84	$[GaCl(thd)]_2$	Ga_2O_2Cl core, tetrahedral	1.890(5) 1.886(5)	94.5(2)		[108]
85	[GaMeCl(acac)]	GaO_2ClR core, tetrahedral	1.901(7) 1.878(7)	96.3(3)		[109]
89	$[GaCl\{N(SiMe3)_2\}(acac)]$	GaO_2ClN core, tetrahedral	1.888(4) 1.881(4)	96.1(2)		[109]
92	$[GaMe_2(hfac)\cdot NC_5H_5]$	GaO_2R_2 core, tetrahedral	1.971(8) 2.590(8)	76.5(3)		[110]
100	$[GaMes_2(hfac)]$	GaO_2R_2 core, tetrahedral	2.008(11) 2.009(11)	88.7(4)		[110]
102	$[GaCl_2(acac)]$	GaO_2Cl_2 core, tetrahedral	1.835(9) 1.835(9)	99.3(6)		[62]
103	$[GaCl_2(thd)]$	GaO2Cl2 core, tetrahedral	1.849(4) 1.841(3)	98.2(1)		[62]
106	$[GaMe_2\{C(OC(4\text{-}OCH_3Ph))_2\}]$	GaO_2R_2 core, tetrahedral	1.921(2) (av.)	93.89(14)		[111]
108	$[GaMe_2(NOC_{13}H_9)]$	$GaONR_2$ core, tetrahedral	1.899(2)	94.10(7)[a]		[111]
127	$[GaMe_2\{OC(Ph)CHC(Me)N(p\text{-methoxyphenyl})\}]$	$GaONR_2$ core, tetrahedral	1.930(4)	93.5(2)[a]		[112]
132	$[GaCl_3\cdot\{O(C(CH_3))_3NHDipp\}]$	$GaCl_3O$ core, tetrahedral	1.864(5)			[113]
133	$[InMe_2\{OC(CH_3)CC(CH_3)N(CH_2)_2NEt_2\}]$	$InON_2R_2$ core, trigonal bipyramidal	2.238(2)	82.61(8)[a]		[113]
27	$[GaEt(OCH_2CH_2NMe_2)_2]$	GaO_2N_2R core, trigonal bipyramidal	1.8522(13) 1.8534(13)	114.94(6)		[104]
134	$[GaCl(OCH_2CH_2NMe_2)_2]$	GaO_2N_2Cl core, trigonal bipyramidal	1.841(2) 1.842(3)	135.08(13)		[115]
135	$[GaCl(OCH(CH_3)CH_2NMe_2)_2]$	GaO_2N_2Cl core, trigonal bipyramidal	1.8372(12) 1.8389(12)	118.91(6)		[115]
136	$[GaMe(O^tBu)_2]_n$	GaO_4R core, trigonal bipyramidal	2.095(1) 1.886(1)	164.98(6) 76.53(5) 94.70(5) 109.43(6)	104.47(6)	[115]
137	$[GaMe(OEt)_2]_n$	GaO_4R core, trigonal bipyramidal	1.896(3) 1.897(3) 2.089(3) 2.094(3)	165.7(1) 109.1(2) 94.9(1) 76.7(1) 77.1(1) 94.5(1)	103.3(1) 102.9(2)	[115]
139	$[Ga(OEt)_3]$	GaO_5 core, trigonal bipyramidal	1.74(1) 1.89(2) 1.98(2) 2.00(2) 2.01(2)	176.8(9) 101.4(8) 79.7(9) 94.5(8) 77.7(8) 97.6(9) 88.4(9) 108.7(9) 125.7(9) 125.2(9)	99.3(8) 102.7(9)	[115]

[a] O–M–N bond angle (°) for β-ketoiminate compounds.

but have not been used as precursors to thin films of gallium and indium oxide. Because this section can be viewed as an update of a previously published 2006 review, we have continued the format followed in that work. To this end, the discussion of the structural and physical properties goes into greater depth than is found in Sections 2 and 3 of this review. Additionally, Table 1 summarised the key bond lengths and angles of crystallographically characterized compounds, which has been organised into four areas: gallium and indium mono(alkoxides, β-diketonates and β-diketoiminates); bis(alkoxides); tris(alkoxides and β-diketonates) and finally cluster compounds of gallium and indium.

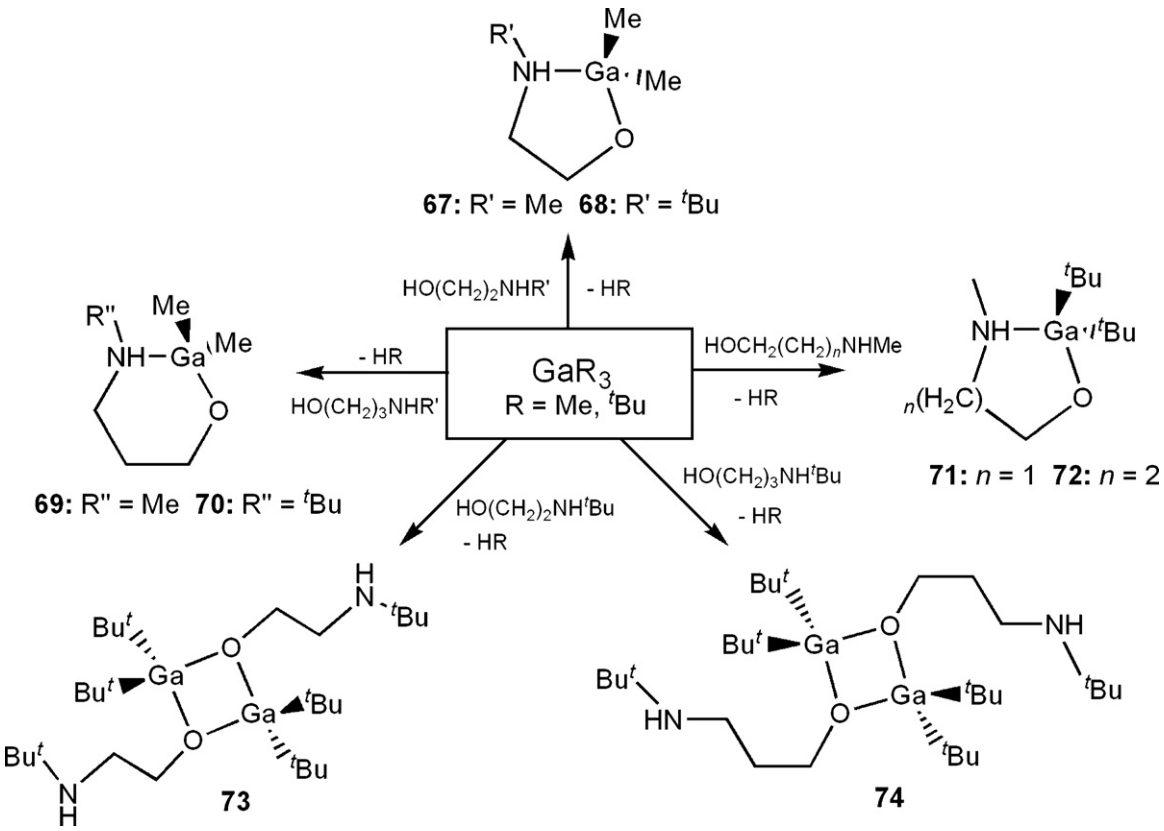

Scheme 20. Synthesis of mono(alkoxides) containing NH groups.

4.1. Mono(alkoxides, β-diketonates and β-diketoiminates)

The reaction of $GaMe_3$ with donor functionalized alcohols $HO(CH_2)_2NHR$ and $HO(CH_2)_3NHR$ (Scheme 20) afforded the gallium mono(alkoxides) $[GaMe_2(O(CH_2)_2NHR)]$ (**67**: R = Me; **68**: R = ^{t}Bu) and $[GaMe_2(O(CH_2)_3NHR)]$ (**69**: R = Me; **70**: R = ^{t}Bu). The reaction of Ga^tBu_3 and the donor functionalized alcohols $HO(CH_2)_nNHMe$ also resulted in the formation of compounds $[Ga^tBu_2(OCH_2(CH_2)_nNHMe)]$ (**71**: $n = 1$; **72**: $n = 2$). Surprisingly, these compounds are monomeric in nature: this is thought to be a result of the presence of a hydrogen atom on the coordinating amine. This enables hydrogen-bonding to a neighbouring alkoxide oxygen to take place, which occurs preferentially over the formation of the Ga_2O_2 ring seen in other gallium mono(alkoxide) compounds (see Section 2.2). IR spectroscopy exhibited a broad N–H absorption, confirming the presence of bridging hydrogen atoms [103].

The molecular structure of compounds **69** and **72** were determined by X-ray crystallography, confirming the presence of 4-coordinate, monomeric complexes with the gallium centre in a distorted tetrahedral geometry [bond angles at gallium range from 94.5(1)° – 122.0(4)° (**69**) and 96.5(1)–122.0(1)° (**72**), Fig. 12]. The Ga–O bond distances [1.875(6) Å (**69**); 1.870(2) Å (**72**)] are comparable to other monomeric gallium alkoxide compounds. Coordination of the nitrogen atom to the gallium centre was observed in both cases [Ga–N bond distance = 2.049(7) Å (**69**); 2.093(2) Å (**72**)]: these are much shorter than the Ga–N bond lengths observed for the dimeric gallium mono(alkoxides) with only two methylene units in the alkoxide (Section 2.2). The reason for this apparent anomaly is not completely understood, but it is believed to be a combination of factors such as the difference in carbon backbone length (three methylene units for **69** and **72** as opposed to two methylene units for **24**), sterics at the gallium centre (Me *vs.* ^{t}Bu) and the electronic effect of the other ligands attached to the gallium centre (methyl groups or chloride anions).

The combination of a bulkier R group on gallium (^{t}Bu) and a bulkier donor functionalized ligand results in the formation of a dimeric compound $[Ga^tBu_2\{O(CH_2)_nNH^tBu\}]_2$ (**73**: $n = 2$; **74**: $n = 3$). Both compounds **73** and **74** contain the expected Ga_2O_2 ring at the heart of the molecule, but in compound **73** the centre of the ring lies on an inversion centre in the unit cell. The gallium atoms in both compounds are in a distorted tetrahedral geometry with the "arm"

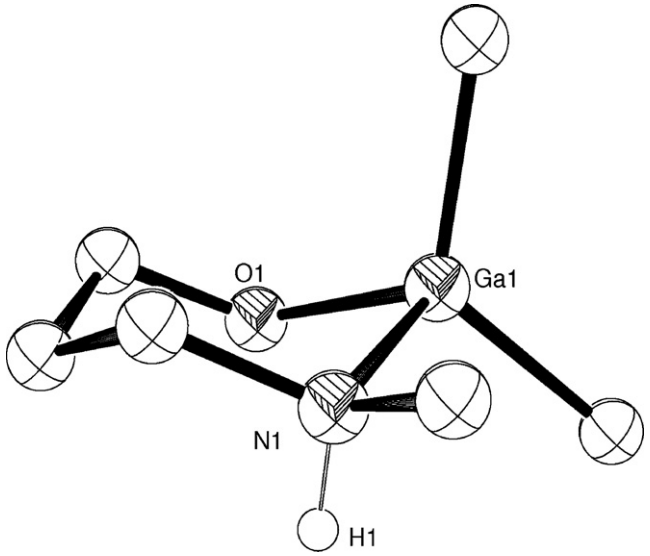

Fig. 12. ORTEP diagram showing the monomeric nature of **69**. H atoms (bar NH) omitted for clarity.

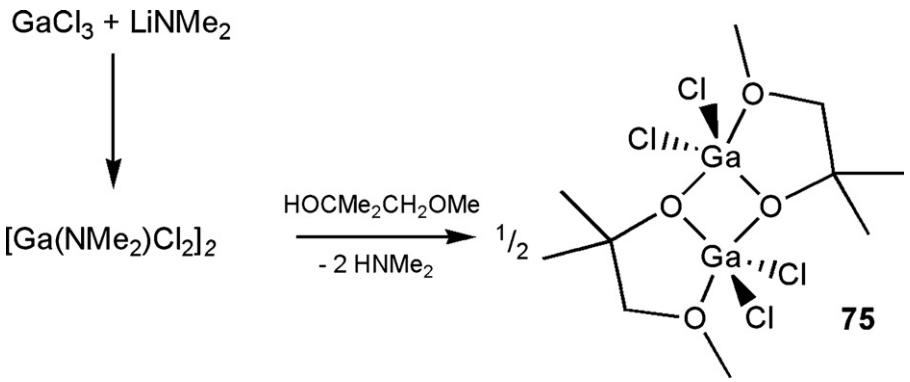

Scheme 21. Synthesis of compound **75**.

of the donor-functionalized alkoxide dangling free, presumably as a result of the steric bulk around the gallium centre. The Ga–O bond lengths [1.95(1)–1.96(1) Å] are significantly longer than those seen in **69** and **70**, which is a consequence of a dimeric structure being adopted.

Gallium mono(alkoxides) can also be reliably synthesised *via* a two step mechanism (Scheme 21). Gallium trichloride is reacted with one equivalent of lithium dimethylamide resulting in the formation of dichlorogallium dimethylamide $[Ga(NMe_2)Cl_2]_n$. Reaction with a single equivalent of the donor functionalized alcohol $HOCMe_2CH_2OMe$ afforded $[GaCl_2(OCMe_2CH_2OMe)]_2$ (**75**) [104]. The structure of **75** was determined by X-ray crystallography which revealed a dimer had been formed with the expected centrosymmetric, planar Ga_2O_2 ring (Fig. 13). Each gallium atom was in a distorted trigonal bipyramidal environment with the centre of the Ga_2O_2 ring lying on an inversion centre in the unit cell. The Ga–O bond lengths within the Ga_2O_2 ring were 1.886(2)–1.975(3) Å, comparable to those seen in **73** and **74**, and the dative Ga–O bonds were much longer at 2.161(3) Å.

The synthesis of a dimeric dialkyl gallium hydroxide compound $[Ga(OH)\{CH(SiMe_3)_2\}_2]_2$ (**76**) was reported by Uhl et al. *via* the reaction of $[Ga_2\{CH(SiMe_3)_2\}_4]$ and water (Scheme 22), and the solid state structure was obtained [105]. The gallium centres adopt a distorted four-coordinate tetrahedral geometry with Ga–O bond lengths of 1.963(4) and 1.976(4) Å, similar to

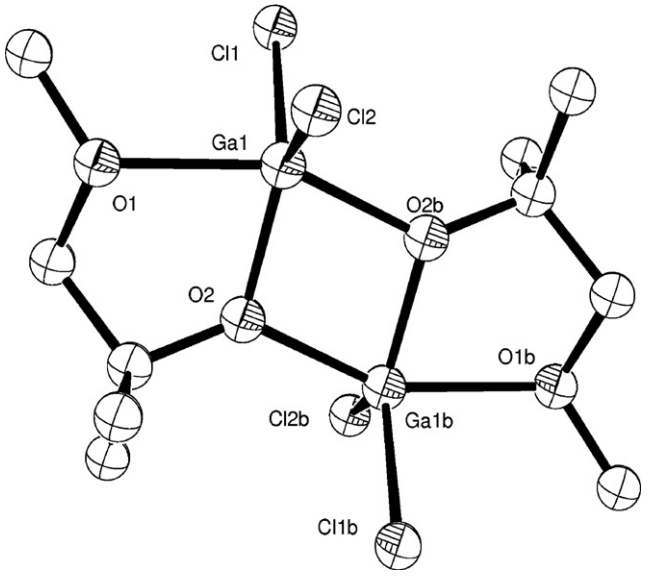

Fig. 13. ORTEP diagram of compound **75**. Hydrogen atoms omitted for clarity.

the digallium halide **75** [106]. The carboxylato-bridged digallane compounds $[Ga(O_2CR)\{CH(SiMe_3)_2\}]_2$ (**77**: R = Ph; **78**: 4-Br-Ph; **79**: 3,5-$C_6H_3Me_2$; **80**: CMe_3) were synthesised by reacting two equivalents of the appropriate carboxylic acid with $[Ga_2\{CH(SiMe_3)_2\}_4]$. A single crystal of **79** was obtained and it was structurally characterized, showing a dimeric compound had formed with the gallium atoms in a distorted four-coordinate tetrahedral environment. Ga–O bond lengths [2.004(6)–2.010(6) Å] are consistent with literature values.

The compound $[M_2\{CH(SiMe_3)_2\}_4]$ was also reacted with two equivalents of Hbzac, resulting in the formation of compounds $[M_2\{CH(SiMe_3)_2\}_2(bzac)_2]$ (**81**: M = Ga; **82**: M = In) [107]. The compounds were confirmed as dimers by spectroscopic analysis, including single crystal X-ray diffraction for compound **81**. The molecule has a *trans* conformation with the crystallographic centre of symmetry located in the middle of the Ga–Ga bond. The gallium atoms are in a distorted four-coordinate tetrahedral geometry and the Ga–O bond lengths average 1.959(3) Å, significantly shorter than the value observed for compound **79**. This is thought to be due to the lack of bridge between the two Ga atoms atoms and also due to less steric stress at the gallium centres.

Beachley et al. have synthesised a number of mono(β-diketonate) compounds of gallium (**83–103**). Dimeric $[Ga_2Cl_4{\cdot}2THF]$ was reacted with two equivalents of [Na(bdk)], affording compounds of the type $[GaCl_2(bdk)]$ (**83**: bdk = acac; **84**: bdk = thd; Scheme 23) [108]. Structural characterization of compounds **83** and **84** was obtained, showing the dimeric nature of **83** and **84**. Both compounds have a direct Ga–Ga bond with each gallium centre in a distorted four-coordinate tetrahedral geometry. The Ga–O bond lengths are similar for both compounds [1.888(6) Å (**83**); 1.889(6) Å (**84**)], in agreement with literature values [49].

Products of formula [GaRCl(acac)] (**85**: R = Me; **86**: R = Et; **87**: R = Mes) were synthesised from the reaction of two equivalents of $[GaRCl_2]$ and Na(acac) (Scheme 24) [109]. Compounds of the type $[GaX\{N(SiMe_3)_2\}(acac)]$ (**88**: R = Me; **89**: R = Cl) were also reported *via* the reaction of [GaRCl(acac)] with $[LiN(SiMe_3)_2]$. Compounds **85–89** are monomeric in the solid state as confirmed by spectroscopic analysis, including single crystal X-ray analysis of **85** and **89**. The gallium centres for both compounds are in a distorted four-coordinate tetrahedral geometry with Ga–O bond lengths [1.901(7) and 1.878(7) Å (**85**); 1.888(4) and 1.881(4) Å (**89**)], in close agreement with literature values.

Beachley et al. also reported the synthesis of the gallium β-diketonate compounds **90–101** using three different routes (Scheme 25) [110]. It was found that the first route was the most successful in producing pure and high yielding products, which were also monomeric in nature. Compounds $[GaMe_2(hfac){\cdot}NC_5H_5]$ (**92**) and $[GaMes_2(hfac)]$ (**100**) were obtained and analysed using

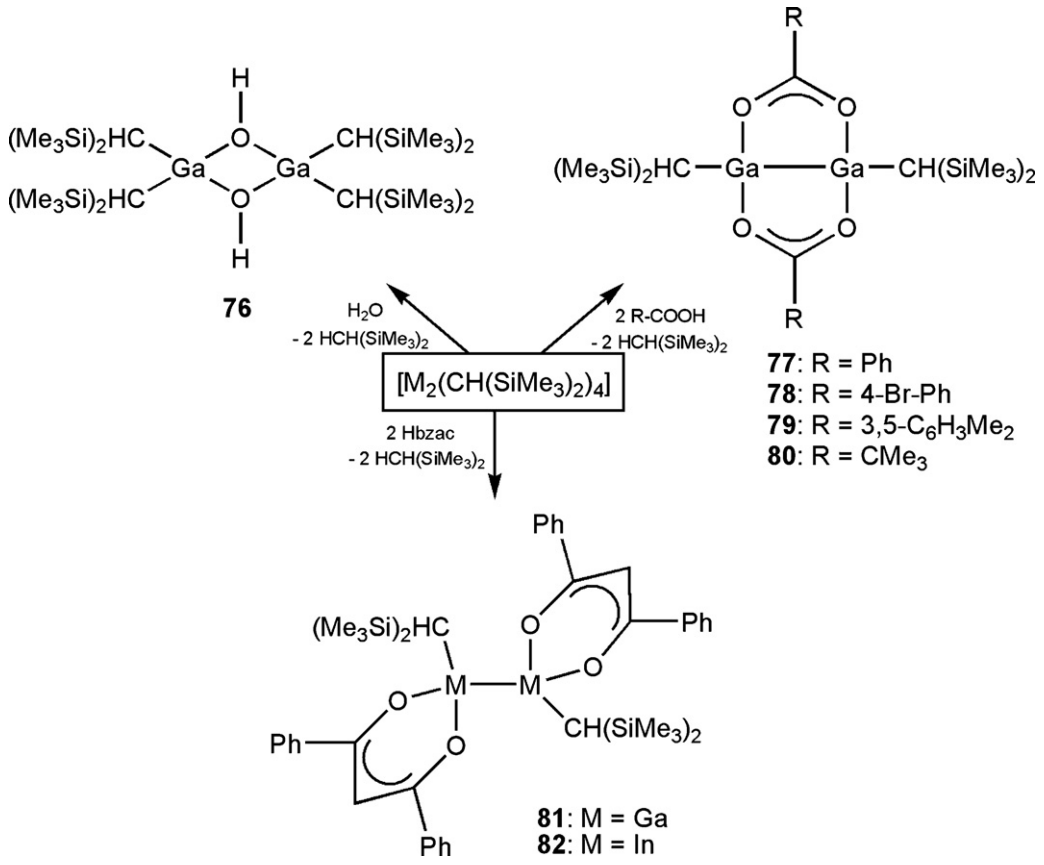

Scheme 22. Synthesis of compounds **76–82**.

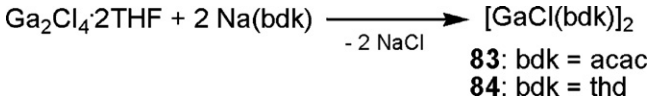

Scheme 23. Synthesis of compounds **83** and **84**.

X-ray crystallography. The gallium centre in both **92** and **100** was in a distorted four-coordinate tetrahedral environment, but the Ga–O bonding was different for the two compounds. Complex **92** has one Ga–O bond consistent with literature values [1.971(8) Å] and one much longer Ga–O bond [2.590(8) Å], which is consistent with a dative interaction, an unusual bonding mode for metal β-diketonates. The Ga–O bond lengths in compound **100** [2.008(11) and 2.009(11) Å], are in agreement with literature values.

The reaction of gallium trichloride with one equivalent of [Na(bdk)] in benzene resulted in the formation of [$GaCl_2$(bdk)] (**102**: bdk = acac; **103**: bdk = thd; Scheme 26) [62]. X-ray crystallographic studies show that both compounds exist as monomers, with the gallium atom in a four coordinate distorted tetrahedral environment. Compound **102** is located on a mirror plane within the unit cell [Ga–O bond length 1.849(4) Å] whereas compound **103** is not, albeit the Ga–O bond lengths are the same within experimental error [1.835(9) and 1.841(3) Å].

The compound [$GaMe_2$(acac)] (**104**) was synthesised by reacting trimethyl gallium with one equivalent of acetylacetone (Scheme 27) [61]. Spectroscopic analysis revealed that compound **104** is monomeric in the solid state.

A range of monomeric gallium β-diketonate complexes (**105–107**), gallium α-(2-pyridyl)acetophenone complexes (**108–110**), gallium *N*-alkylaldimine complexes (**111–115**), gallium N,O-bidentate complexes (**116–117**) and gallium *N*-arylaldimine complexes (**118–125**) have been reported (Scheme 28) [111]. Compounds **105–125** were synthesised by the reaction of [$GaMe_2OH$] and the relevant ligand. The compounds were analysed using spectroscopic methods and mass spectroscopy confirmed the compounds to be monomeric in nature. Single crystals of **106**

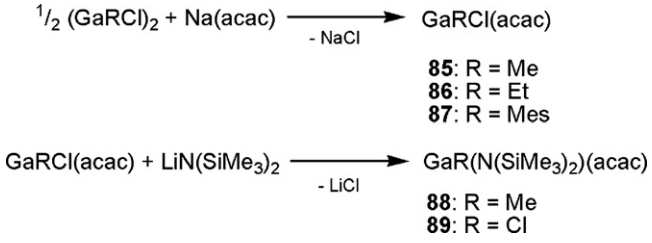

Scheme 24. Synthesis of compounds **85–89**.

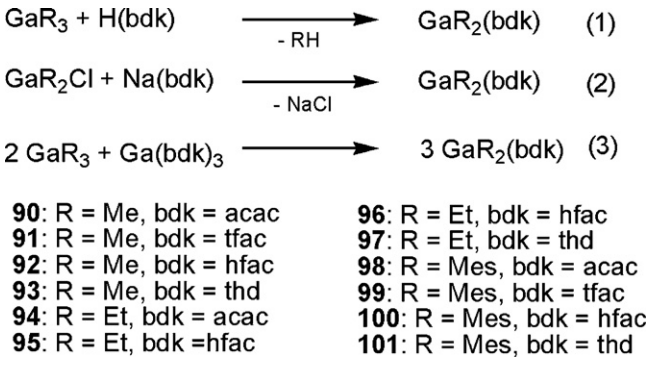

Scheme 25. Synthesis of compounds **90–101** *via* three different routes.

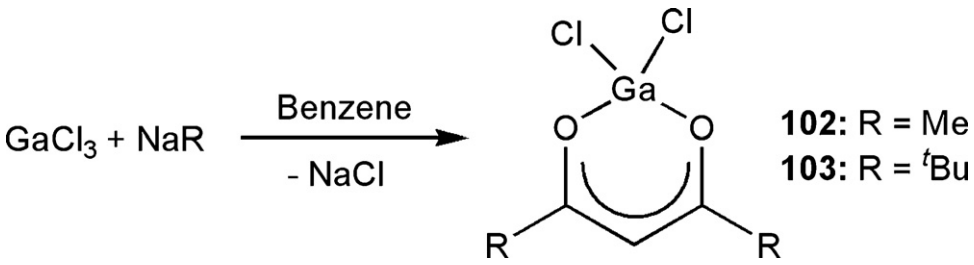

Scheme 26. Synthesis of compounds **102** and **103**.

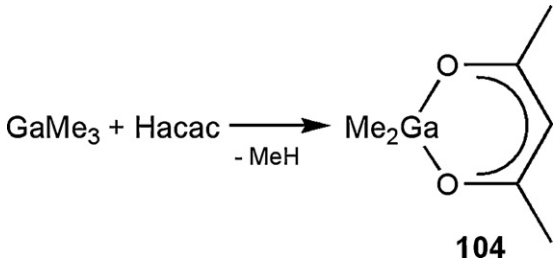

Scheme 27. Synthesis of compound **104**.

and **108** confirmed a four-coordinate distorted tetrahedral environment for the gallium centres. The average Ga–O bond lengths [1.921(2)Å (**106**) and 1.899(2) (**108**)] are in agreement with literature values.

Formation of the dimethyl gallium β-ketoiminate compounds **126–131** was accomplished by reacting MMe_3 (M = Ga, In) with a single equivalent of the appropriate β-ketoimine ligand (Scheme 29) [112].

Compounds **126–131** were isolated as yellow solids, with mass spectrometry indicating the monomeric nature of these complexes. Single crystals of compound **127** were obtained and analysed by X-ray diffraction, which confirmed the monomeric structure of **127**. The gallium centre is in a distorted four-coordinate tetra-

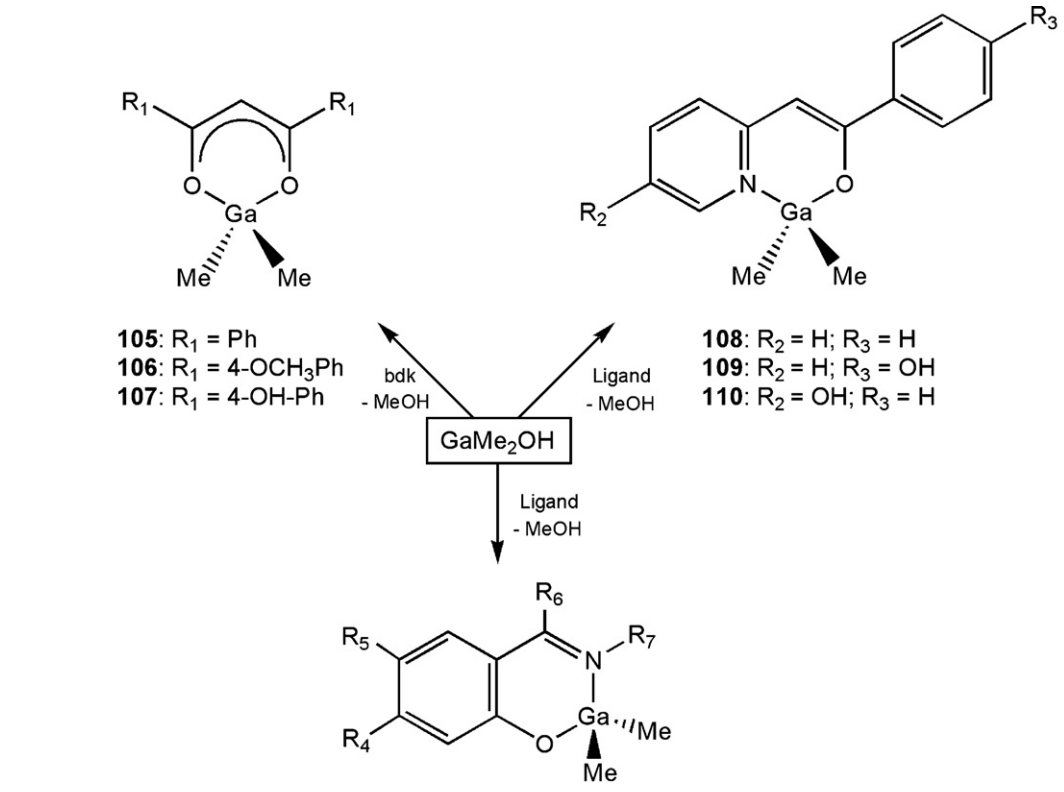

Scheme 28. Synthesis of compounds **105–125**.

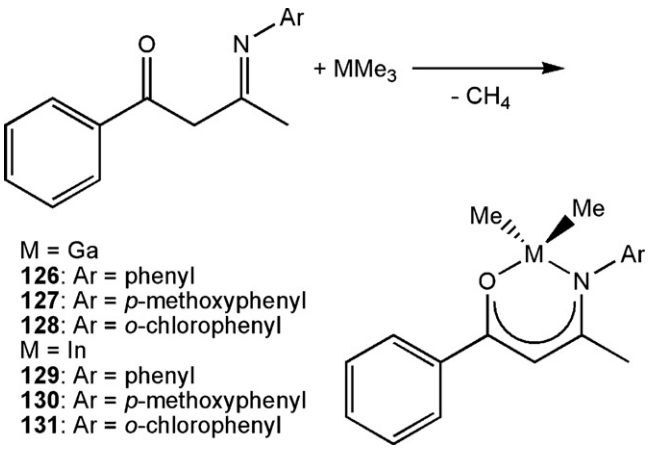

Scheme 29. Synthesis of compounds **126–131**.

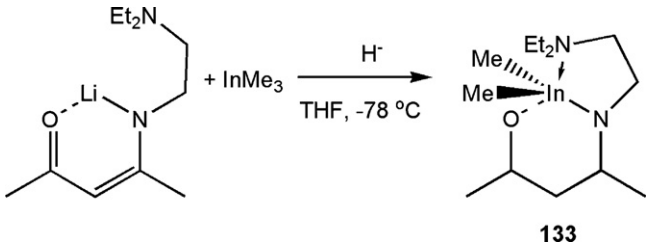

Scheme 31. Synthesis of compound **133**.

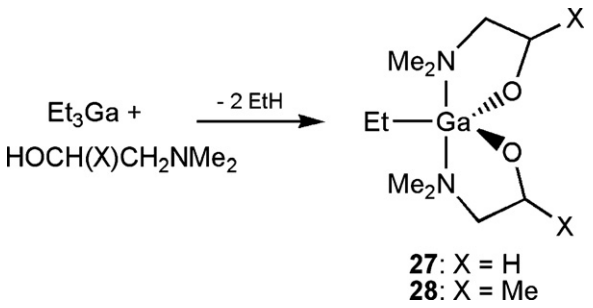

Scheme 32. Synthesis of compounds **27** and **28**.

hedral geometry due to the crowded environment around the gallium-bound O and N atoms. The Ga–O bond length [1.930(4) Å] is consistent with literature values for sterically bulky compounds. The Ga–N bond length [2.201(4) Å] is characteristic of a dative Ga–N bond, as seen with gallium donor functionalized alkoxides.

The compound $[GaCl_3\{O(C(CH_3))_3NHDipp\}]$ (**132**) was synthesised from the reaction of $GaCl_3$ with the lithiated β-ketoiminate (Scheme 30) [113]. Salt metathesis is expected for these types of reactions, but in this case a ligand-metal adduct was isolated as low yielding (20%) colourless crystals. The gallium centre is in a distorted four-coordinate tetrahedral environment and the Ga–O bond length [1.864(5) Å] is in agreement with literature values for Ga–O bonds.

The reaction of a 1:1 ratio of $InMe_3$ and the lithiated β-ketoiminate (Scheme 31) afforded colourless crystals of $[InMe_2\{OC(Me)CHC(Me)N(CH_2)_2NEt_2\}]$ (**133**), which was characterized using X-ray analysis. The indium centre is in a distorted 5-coordinate trigonal bipyramidal geometry with direct bonds to the two methyl groups and the central nitrogen [In–N bond length 2.242(2) Å], a partial bond to the oxygen [In–O: 2.238(2) Å] and a dative bond to the terminal nitrogen [In–N: 2.538(2) Å], which are similar to those reported in larger indium cluster compounds [114].

4.2. Bis(alkoxides)

Gallium and indium bis(β-diketonate) and bis(β-ketoiminate) complexes are unknown, and bis(alkoxides) are rare in comparison to the mono(alkoxide) complexes of these elements. A series of mono, bis and tris gallium alkoxides were synthesised by Basharat et al. and a number of the mono and tris gallium alkoxides were used for the deposition of Ga_2O_3 (Section 2.2) [57].

The gallium bis(alkoxides) $[GaEt(OCH(X)CH_2NMe_2)_2]$ (**27**: X = H; **28**: X = Me, Scheme 32) were not used to deposit gallium oxide thin films and resulted from the reaction of $GaEt_3$ and excess donor-functionalized alcohol. Compounds **27** and **28** were characterized using spectroscopic methods and **27** was also characterized by single crystal X-ray diffraction, which confirmed a monomeric structure. The gallium centre is in a distorted five-coordinate square-based pyramidal geometry with the apical ligand being the ethyl group. The Ga–O bond lengths [1.8522(13) and 1.8534(13) Å] and the Ga–N bonds [2.269(15) and 2.2675(14) Å] are in agreement with other gallium bis(alkoxide) complexes.

As described above (Section 4.1), adding equimolar equivalents of alcohol to MR_3 (M = Ga, In) resulted in the mono(alkoxides) $[MR_2(OR')]_n$. However, the reaction of these species with two equivalents of alcohol does not reliably afford the expected gallium or indium bis(alkoxide) $[MR(OR')_2]$. A successful synthetic route to gallium bis(alkoxides) is realised by first synthesising chlorogallium bis(dimethylamide), $[Ga(NMe_2)_2Cl]_2$, before the addition of two equivalents of donor-functionalized alcohol (Scheme 33) affords the gallium bis(alkoxides) $[GaCl(OCH_2CH_2NMe_2)_2]$ **134** and $[GaCl(OCHMeCH_2NMe_2)_2]$ **135** [104].

The structures of **134** and **135** (Fig. 14) were determined by single crystal X-ray diffraction. Both compounds are monomeric in the solid state, with the gallium centre in a 5-coordinate, distorted trigonal bipyramidal environment. The two oxygen atoms and the chlorine atom occupy the equatorial positions in both compounds, with the two nitrogen atoms in the axial positions. The N–Ga–N angles [165.55(11)° (**134**) and 168.80(6)° (**135**)] are similar. The Ga–O bond lengths [1.841(2) and 1.842(3) Å (**134**); 1.837(3) and 1.838(9) Å (**135**)] are consistent with other gallium alkoxides. The Ga–N bond lengths [2.161(3) and 2.118(3) Å (**136**); 2.151(6) and 2.168(1) Å (**137**)] are also consistent with previously observed compounds.

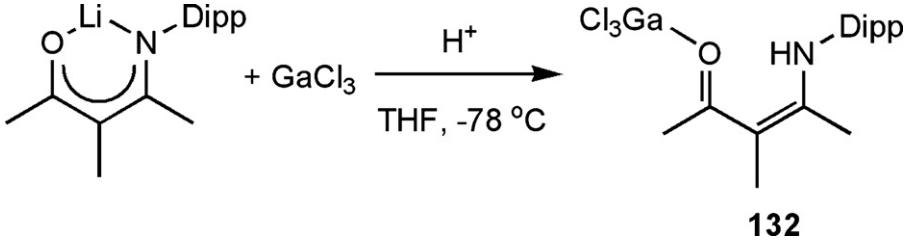

Scheme 30. Synthesis of compound **132**.

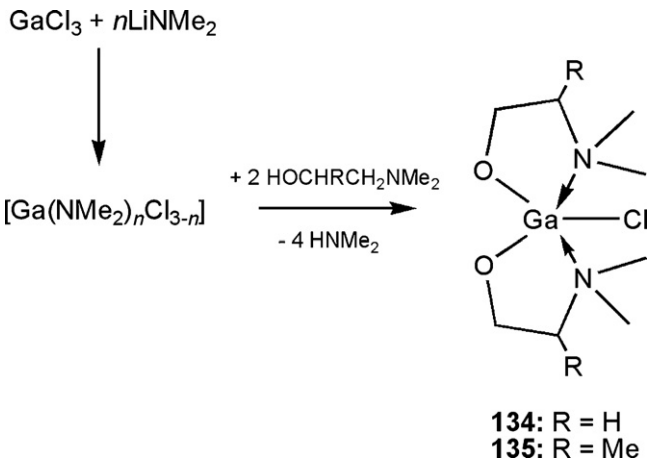

Scheme 33. Synthesis of compounds **134** and **135**.

The reaction of trimethyl gallium with two equivalents of ROH in hot toluene (Scheme 34) resulted in the formation of the dimeric gallium bis(alkoxides) $[GaMe(OR)_2]_2$ (**136**: R = ^{t}Bu; **137** and **138**; R = Et) [115]. When R = ^{t}Bu, only the *trans* isomer is formed (**136**), however when R = Et, both the *trans* (**137**) and the *cis* (**138**) isomers are formed in a 1.2:1 ratio. In the solid state, crystals of **136** and **137** were obtained and analysed using X-ray analysis. Compounds **136** and **137** exist in a polymeric form where each gallium centre is in a distorted 5-coordinated trigonal bypyramidal environment, bonding to four bridging OEt groups and a single methyl group. The Ga–O bond lengths [2.095(1) and 1.886(1) Å (**136**); 1.896(3), 1.897(3), 2.089(3) and 2.094(3) Å (**137**)] are consistent with other compounds of this nature [103].

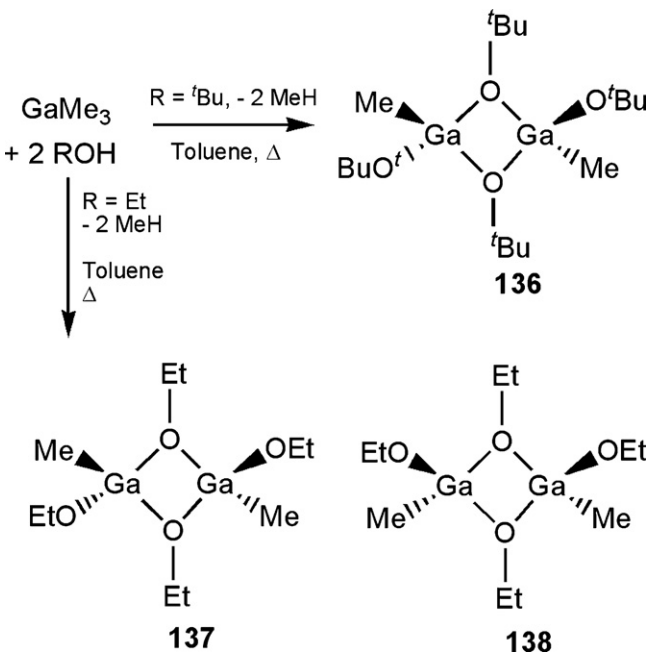

Scheme 34. Synthesis of compounds **136–138**.

4.3. Tris(alkoxides) and β-diketonates

A range of simple gallium tris(alkoxides) (**1**, **30**, **138–140**) have been synthesised *via* an electrochemical method, utilising a metallic gallium anode and the appropriate alcohol (Scheme 35) [116]. This resulted in the formation of $[Ga(OR)_3]_n$ (**138**: R = Me; **139**: R = Et; **1**: R = ^{i}Pr; **140**: R = ^{n}Bu; **30**: R = CH_2CH_2OMe). The cathode was a platinized platinum plate and Bu_4NBr, Et_3BzNCl or LiCl were used as an electroconductive additive in the alcohol. X-ray diffraction patterns were obtained for powders of **139**, in addition to single crystal X-ray diffraction analysis. This showed a 1D-polymer of zig–zag chains of gallium centres, each in a distorted 5-coordinated trigonal bipyramidal geometry which was bound to four bridging and a single terminal OEt group. The Ga–O bond length for the terminal OEt group [1.74(1) Å] and the longer, bridging Ga–O bond lengths [1.89(2), 1.98(2), 2.00(2) and 2.01(2) Å] are all consistent with previously observed compounds.

A series of metal tris(β-diketonate) compounds have been reported over the years and many of these have been used to deposit gallium and indium oxide thin films (see Sections 2.3 and 3.3). A range of gallium and indium tris(β-diketonates) were synthesised (compounds **38**, **39**, **61–63**, **141–168**) *via* the reaction of metal nitrate with stoichiometric amounts of β-diketonate (Scheme 36) [117].

Compounds **141**, **152** and **165** were isolated as oils and characterized using spectroscopic methods, the remaining compounds were all isolated as solids. No single crystal X-ray analysis was carried out.

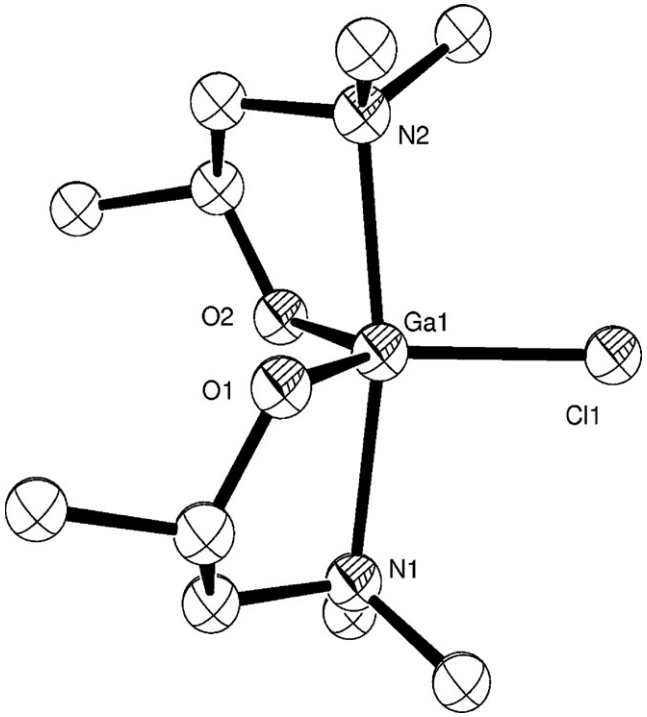

Fig. 14. ORTEP diagram of $[GaCl(OCHMeCH_2NMe_2)_2]$ **135**. H atoms omitted for clarity.

4.4. Clusters

Multinuclear metal alkoxides could be used as precursors to metal oxide films because they contain preformed metal–oxygen bonds, although they do not necessarily have the correct M:O ratio.

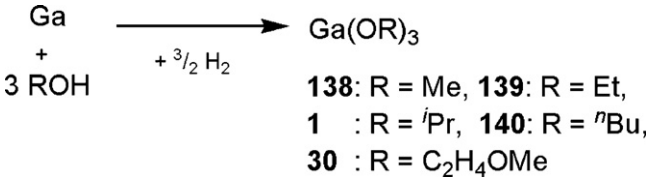

Scheme 35. Synthesis of compounds **1**, **30**, **138–140** *via* an electrochemical method.

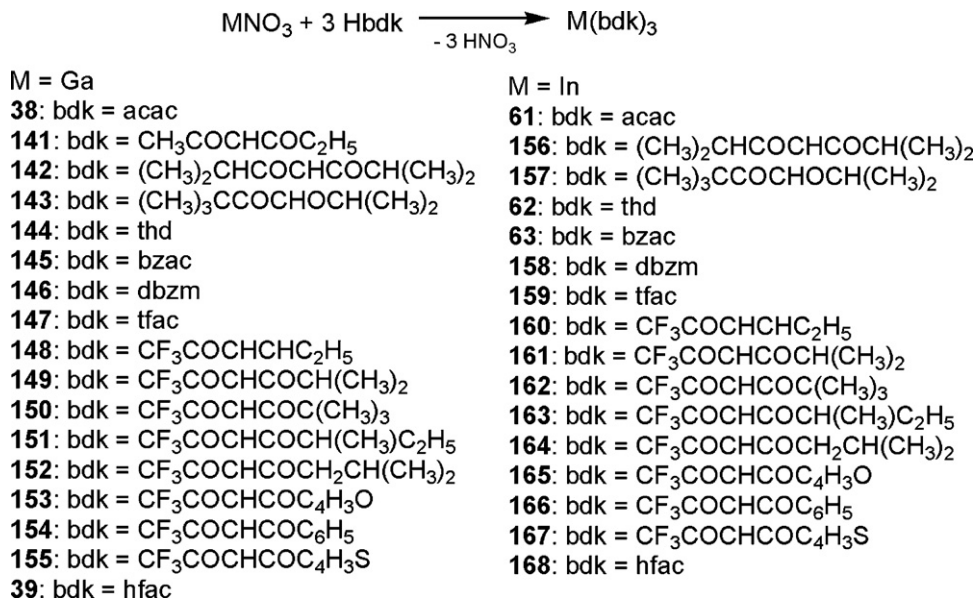

Scheme 36. Synthesis of compounds **38**, **39**, **61–63**, **141–168**.

Ziemkowska et al. reported the formation of trinuclear gallium (**169**) and indium (**170**) metal alkoxide clusters from the synthesis of MMe_3 (M = Ga, In) with benzopinacol (Scheme 37) [114]. The structure of **169** was determined by single crystal X-ray diffraction analysis.

The structure has two Ga_2O_2 four-membered rings and two GaO_2C_2 five-membered rings that make up a tetracyclic centre. The central Ga atom has a distorted five coordinate square based pyramidal geometry. The oxygen atoms form the basal coordination plane and the methyl group occupies the apical position. The terminal Ga–O bond lengths [1.965–1.994 Å] are consistent with literature examples which have large steric bulk around the gallium centre. Presumably due to crystal packing effects, the coordination environment around the central gallium cation is distorted away from ideal. This is manifested in the central Ga–O bond lengths whereby two of the *trans* bond lengths are elongated [Ga–O 2.013(3) and 1.986(3) Å] and two are compressed [Ga–O 1.924(3) and 1.932(3) Å].

Although the indium cluster **171** was not crystallographically characterized, the reaction of benzopinacol with $InMe_3$ and [$InMe_2OMe$] in a 1:1:1 ratio afforded compound **171** (Scheme 38). The centrosymmetric, tetranuclear molecule **171** has three In_2O_2 four-membered rings and two InO_2C_2 five-membered rings making up a pentacyclic structure. The central indium atoms are in a five-coordinate square-based pyramidal geometry with the oxygen atoms in the basal positions and the methyl group in the apical position. The In–O bond lengths vary between 2.155–2.219 Å, longer than other literature examples, but bond elongation is expected where the metal centre experiences steric crowding from surrounding ligands [74,118,119].

Compound **172** is an example of a self-assembled, supramolecular, high-symmetry metal-ligand cluster (Scheme 39) [120]. Equimolar quantities of [$Ga(acac)_3$] are added to ligand H_3L and after a period of 16 h at 90 °C, a microcrystalline material **172** was isolated. The compound was analysed using ^1H NMR and ^{13}C NMR and the structure confirmed by single-crystal X-ray diffraction. The structure shows the self-assembled cluster to have a cylindrical geometry where each gallium atom defines a distorted trigonal antiprism, in which six ligands make up the equatorial faces of the cylinder with a hole at the bottom and the top.

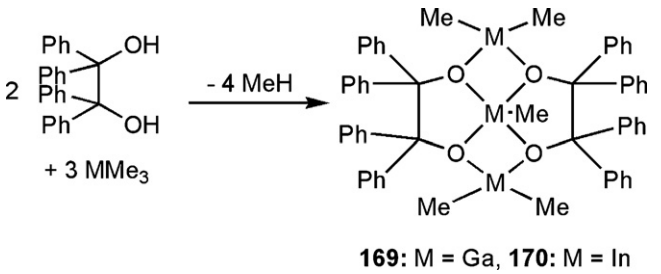

Scheme 37. Synthesis of compounds **169** and **170**.

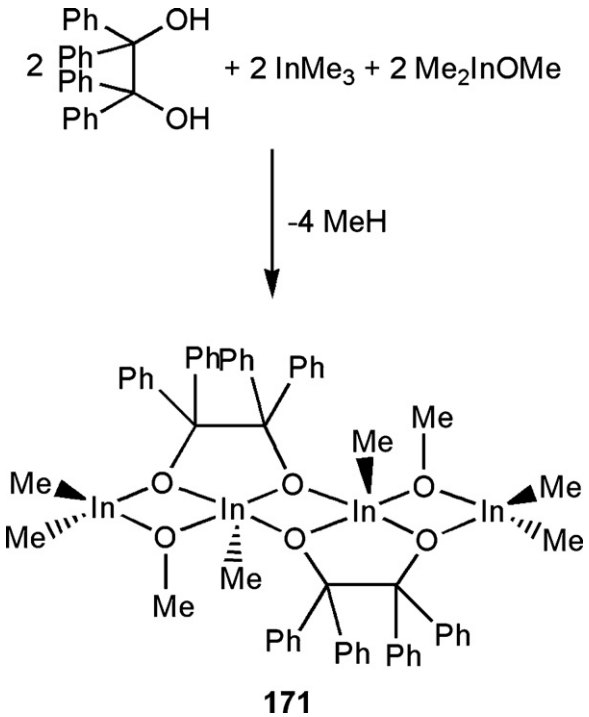

Scheme 38. Synthesis of compound **171**.

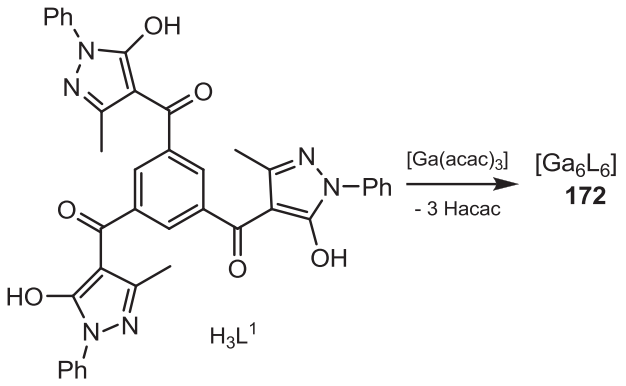

Scheme 39. Synthesis of compound **172**.

Albrecht et al. have synthesised gallium bis(bdk) compounds $Ga_2(L^1)_3$ (**173**) [121] and $Ga_2(L^2)_3$ (**174**) and $[Ga_9(L^2)_8(OH)_{10}]NO_3$ (**175**) [122] *via* the reaction of gallium nitrate with β-diketones (Scheme 40). For compound **173** the reactants self-assemble in solution and form the dinuclear helicate-type cryptand regardless of the M:L ratio. The three ligands in **173** bridge the gallium centres, resulting in an octahedral coordination geometry at gallium. The Ga–O bond lengths [1.935–1.975 Å] are consistent with literature values for gallium compounds with bulky ligands. Following the same method with bis-β-diketonate L^2, compound **174** is formed. It was characterized by mass spectrometry and NMR spectroscopy, but could not be isolated as a pure product indicating it does not form by strict self-assembly. The reaction was repeated in wet methanol and resulted in the formation of **175**, which was crystallographically characterized. The solid state structure revealed the compound has an inner nonanuclear gallium hydroxide cluster surrounded by eight ditopic ligands of L^2 where two gallium centres are bridged by hydroxyl groups and two ligands wrap around the metal atoms. The Ga–O bond lengths for **175** [1.91–2.05 Å] are characteristic of gallium atoms affected by sterically bulky ligands. The larger range in bond length discrepancy can be caused by packing effects in the solid state.

Suslova et al. reported the attempted synthesis of $[Ga(OEt)_3]$ *via* the metathesis of $GaCl_3$ with NaOEt/EtOH in a 1:3 ratio. However, crystals of $[Ga_5(\mu_5\text{-}O)(\mu\text{-}OEt)_8Cl_5]$ (**176**) and $[Ga_{12}(\mu_4\text{-}O)_2(\mu_3\text{-}O)_5(\mu\text{-}OEt)_{10}Cl_{12}(py)_4]$ (**177**) were isolated rather than the expected gallium tris(alkoxide) [123]. Compound **176** was recrystallised from a toluene/MeCN mixture and was characterized by single crystal X-ray diffraction (Fig. 15). The cluster is composed of a flattened tetragonal pyramid of metal atoms, Ga_5, with an octahedrally coordinated $[Ga(\mu_5\text{-}O)(\mu\text{-}OEt)Cl]$ in the axial position and the trigonal bipyramidally coordinated $[Ga(\mu_5\text{-}O)(\mu\text{-}OEt)Cl]$ in the equatorial plane of the pyramid. A pentadentate oxo group is situated in the centre of the pyramid and all its edges are capped by bridging OEt groups. The Ga–O bond lengths [1.931–2.162 Å] are vastly different, which can be explained by the different environments of the gallium atoms. Compound **176** was recrystallised from a toluene/pyridine mixture and characterized by single crystal X-ray diffraction. The structure comprises two octahedrally coordinated gallium atoms, seven trigonal bipyramidally coordinated gallium atoms and three tetrahedrally coordinated gallium atoms. These different gallium atom environments account for the large differences in the Ga–O bond lengths [1.804–2.367 Å].

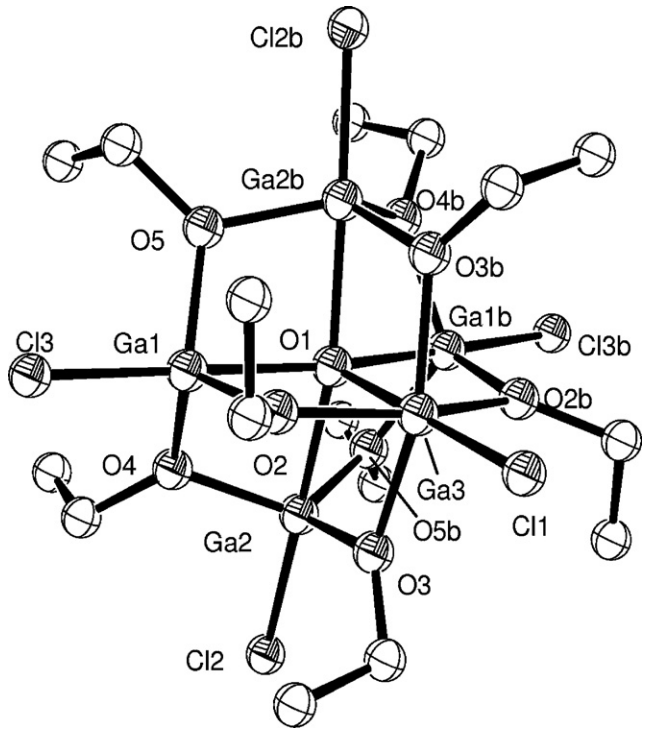

Fig. 15. ORTEP diagram of compound **176**. H atoms omitted for clarity.

A series of tetrahedral indium-containing complexes have been reported by Saalfrank et al. which include mixed metal complexes and indium cationic species which are unsuitable in group 13 metal oxide precursor chemistry [124]. Compound **177** $[In_4(L)_4]$ was synthesised *via* the reaction of $[In(ClO_4)_3]$ with H_3L and triethylamine (Scheme 41). Spectroscopic and X-ray analysis indicated that in the solid-state, the structure of **177** consists of four indium metal centres in a tetrahedral arrangement. Each indium centre is in an octahedral coordination environment, coordinating to three lig-

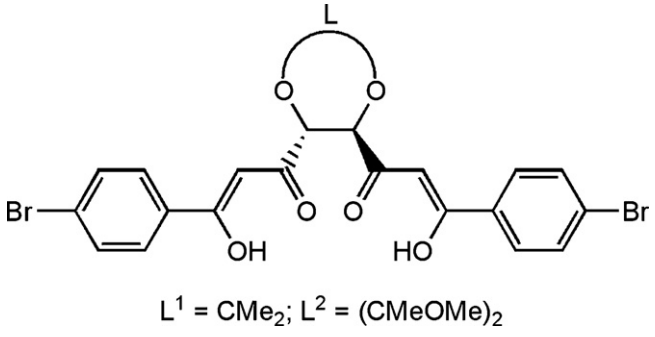

Scheme 40. Diagram showing ligands H_2L^1 and H_2L^2 reacted with gallium nitrate to produce compounds $[Ga_2(L^1)_3]$ (**173**), $[Ga_2(L^2)_3]$ (**174**) and $[Ga_9(L^2)_8(OH)_{10}]NO_3$ (**175**).

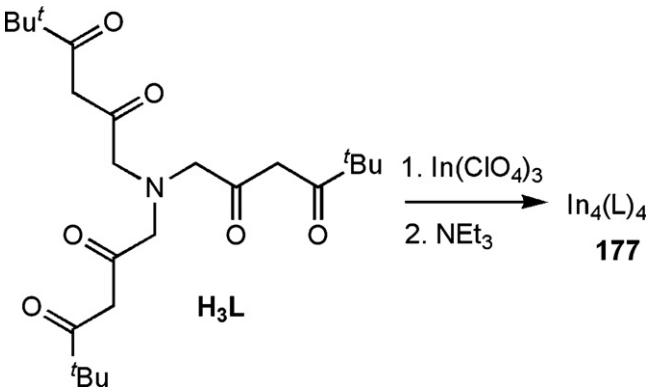

Scheme 41. Synthesis of compound **177**.

ands *via* one of the β-diketonate groups. The In–O bond lengths [2.104(3)–2.161(3) Å] are consistent with other indium cluster compounds.

5. Conclusion

This review has covered the synthesis and characterization of single-source precursors to gallium and indium oxide, and the methods used to deposit gallium and indium oxide thin films. Also included in this review was a section on potential precursors to gallium and indium oxide films, which updates a review previously published in 2006.

Most commonly, metal alkoxide and β-diketonate compounds have been used as precursors to these materials, with commercially available precursors receiving much attention. The composition and structure of the deposited film is greatly affected by the type, nature and purity of the precursor employed since the key step for the formation of the film is the decomposition of the precursor. The type of ligand in the precursor is therefore very important since ideally the ligands associated with the precursor should be cleanly lost in the gas phase during the decomposition process. More complex ligands can result in a complicated fragmentation process taking place during decomposition. A range of gallium and indium singe-source precursors have been described above and most have been successfully employed for the deposition of thin films of indium and gallium oxide. Many of the indium precursors are rather involatile and must be heated to high temperatures to achieve vaporisation of the complex. Indeed, many single-source precursors have low volatilities, however this can be overcome either by using solution-based deposition methods or *via* chemical modification. Common methods of deposition using single-source precursors include chemical vapour deposition (CVD), sol–gel and spin coating methods.

A comparison of precursors is difficult since most were used under different conditions, for example LPCVD versus spin coating. However, the common methods of deposition were successful in producing stoichiometric metal oxide thin films. These methods will continue to be used to improve film qualities, such as conductivity and transparency, as new single-source precursors are synthesised and reported. This review has also shown that there is no one compound which acts as a general "ideal" precursor because each deposition technique has different requirements which are best met by different precursors, e.g. volatility, solubility. A compound that affords clean, stoichiometric films under the conditions of one technique may not even undergo deposition when used in a different technique. Ideally precursors should be able to be synthesised in as few a synthetic steps as possible and be adaptable to larger scale production without major cost implications. Based on these requirements the deposition of gallium and indium oxide films *via* the *in situ* reaction of trialkyl-gallium or indium with donor functionalised alcohols *via* solution-based CVD represents a straightforward route since it involves commercially available reagents and could be compatible with a range of deposition techniques. The deposition conditions, such as temperature, precursor concentration and reaction time will all play an important role in determining the morphology of the resulting material and the level of contamination (e.g. from carbon) in the metal oxide. This can have a crucial effect on the gas sensing and TCO applications of the materials.

Precursor design represents a significant challenge which will be important in the future of thin film production: there is a need to create compounds with preformed M–O bonds, but also compounds that will undergo clean decomposition under the deposition conditions. Another consideration is if the precursors are to be employed in solution based processes, then they should be highly soluble. However, these precursors should also be easily synthesised in high-yielding reactions to be suitable for scale-up in industrial processes. Careful consideration of both the nature of the oxygen-containing group(s) and the other ligands attached to the metal centre should lead to exciting reports of new and optimised single-source precursors appearing in the near future. Furthermore, initial results have indicated that single-source routes could be extended to the formation of doped-gallium or doped-indium oxide, such as the formation of gallium-doped indium oxide.

As more flexible devices are required to incorporate into a range of applications, such as flexible displays for e-readers and OLEDs, flexible barrier layers such as TCOs will be in demand. Currently, TCOs are widely used for rigid devices but the technology used to coat rigid substrates (i.e. glass) is not always applicable for coating flexible substrates. Solution-based processes are ideal for coating flexible substrates and here the development of soluble single-source precursors will play a crucial role. Given the importance of gallium and indium oxide films for TCO applications the formation of precursors is anticipated to continue with the objective of developing cost-effective routes with lower temperature processing.

Acknowledgements

We would like to thank the EPSRC for funding (LGB and DP), grant no. EP/F035675/1.

References

[1] M.G. Blamire, J.L. MacManus-Driscoll, N.D. Mathur, Z.H. Barber, Adv. Mater. 21 (2009) 3827.
[2] K. Seshan, Handbook of Thin Film Deposition, 2nd ed., Noyes Publications, Norwich, 2002.
[3] S. Basharat, C.J. Carmalt, R. Binions, R. Palgrave, I.P. Parkin, Dalton Trans. (2008) 591.
[4] M. Fleischer, H. Meixner, Sens. Actuators B 13 (1993) 259.
[5] Z. Liu, T. Yamazaki, Y. Shen, T. Kikuta, N. Nakatani, Y. Li, Sens. Actuators B 129 (2008) 666.
[6] M. Fleischer, H. Meixner, Sens. Actuators B 5 (1991) 115.
[7] M. Fleischer, H. Meixner, Sens. Actuators B 4 (1991) 437.
[8] H.L. Ma, D.W. Fan, Chin. Phys. Lett. 26 (2009) 117302.
[9] S.C. Vanithakumari, K.K. Nanda, Adv. Mater. 21 (2009) 3581.
[10] S. Daniele, D. Tcheboukov, L.G.H. Pfalzgraf, J. Mater. Chem. 12 (2002) 2519.
[11] A.C. Taş, P.J. Majewski, F. Aldinger, J. Am. Ceram. Soc. 83 (2000) 2954.
[12] P. Meriaudeau, C. Naccache, J. Mol. Catal. 59 (1990) L31.
[13] X. Lai, D. Wang, N. Han, J. Du, J. Li, C. Xing, Y. Chen, X. Li, Chem. Mater. 22 (2010) 3033.
[14] J. Frank, A. Fleischer, A. Zimmer, H. Meixner, IEEE Sens. J. 1 (2001) 318.
[15] R.J. Cava, J.M. Phillips, J. Kwo, G.A. Thomas, R.B.v. Dover, S.A. Carter, J.J. Krajewski, W.F. P Jr., J.H. Marshall, D.H. Rapkine, Appl. Phys. Lett. 64 (1994) 2071.
[16] J.M. Phillips, J. Kwo, G.A. Thomas, S.A. Carter, R.J. Cava, S.Y. Hou, J.J. Krajewski, J.H. Marshall, W.F. Peck, D.H. Rapkine, R.B. van Dover, Appl. Phys. Lett. 65 (1994) 115.
[17] C.G. Granqvist, A. Hultåker, Thin Solid Films 411 (2002) 1.
[18] H.L. Hartnagel, A.L. Dawar, A.K. Jain, C. Jagadish, Semiconducting Transparent Thin Films, IOP Publishing, Bristol, 1995.
[19] T. Maruyama, K. Fukui, Jpn. J. Appl. Phys. 29 (1990) L1705.
[20] R. Nomura, K. Konishi, H. Matsuda, J. Electrochem. Soc. 138 (1991) 631.
[21] K.R. Reyes-Gil, E.A. Reyes-Garcia, D. Raftery, J. Phys. Chem. C 111 (2007) 14579.
[22] Y. Sakata, Y. Matsuda, T. Yanagida, K. Hirata, H. Imamura, K. Teramura, Catal. Lett. 125 (2008) 22.
[23] R. Street, Technology and Applications of Amorphous Silicon, Springer, New York, 2000.
[24] C.G. Granqvist, Sol. Energy Mater. Sol.Cell 91 (2007) 1529.
[25] F. Zhuge, L.P. Zhu, Z.Z. Ye, D.W. Ma, J.G. Lu, J.Y. Huang, F.Z. Wang, Z.G. Ji, S.B. Zhang, Appl. Phys. Lett. 87 (2005) 092103.
[26] J.G. Lu, Z.Z. Ye, F. Zhuge, Y.J. Zeng, B.H. Zhao, J.Y. Huang, Appl. Phys. Lett. 85 (2004) 3134.
[27] J.G. Lu, Z.Z. Ye, L. Wang, B.H. Zhao, J.Y. Huang, Chin. Phys. Lett. 19 (2002) 1494.
[28] Y.R. Ryu, W.J. Kim, H.W. White, J. Cryst. Growth 219 (2000) 1529.
[29] S. Basharat, C.J. Carmalt, S.A. Barnett, D.A. Tocher, H.O. Davies, Inorg. Chem. 46 (2007) 9473.
[30] J.-H. Park, G.A. Horley, P. O'Brien, A.C. Jones, M. Motevalli, J. Mater. Chem. 11 (2001) 2346.
[31] R. Binions, C.J. Carmalt, I.P. Parkin, K.F.E. Pratt, G.A. Shaw, Chem. Mater. 16 (2004) 2489.
[32] L. Heeju, K. Kunhee, W. Jeong-Jun, J. Doo-Jin, P. Youngsoo, K. Yunsoo, L. Hong Won, C. Yong Jai, C. Hyun Mo, ECST 25 (2009) 587.

[33] O. Nilsen, R. Balasundaraprabhu, E.V. Monakhov, N. Muthukumarasamy, H. Fjellvåg, B.G. Svensson, Thin Solid Films 517 (2009) 6320.
[34] F. Shi, S. Zhang, C. Xue, J. Alloys Compd. 498 (2010) 77.
[35] N. Joo Hyon, R. Seung Yoon, J. Sung Jin, K. Chang Su, S. Sung-Woo, P.D. Rack, K. Dong-Joo, B. Hong Koo, Electron. Device Lett. 31 (2010) 567.
[36] S. Mishra, S. Daniele, S. Petit, E. Jeanneau, M. Rolland, Dalton Trans. (2009) 2569.
[37] M.A. Flondoza, R. Castanedo-Perez, G. Torres-Delgado, J. Marquez Marin, O. Zelaya-Angel, Thin Solid Films 517 (2008) 681.
[38] H. Jianhua, C. Michael, J. Phys. D: Appl. Phys. 35 (2002) 433.
[39] G. Korotcenkov, V. Brinzari, M. Ivanov, A. Cerneavschi, J. Rodriguez, A. Cirera, A. Cornet, J. Morante, Thin Solid Films 479 (2005) 38.
[40] E. Shigeno, S. Seki, K. Shimizu, Y. Sawada, M. Ogawa, A. Shida, M. Ide, A. Yajima, A. Yoshinaka, Surf. Coat. Technol. 169–170 (2003) 566.
[41] R. Binions, C.J. Carmalt, I.P. Parkin, Meas. Sci. Technol. 18 (2007) 190.
[42] W.Y. Chung, J. Mater. Sci.-Mater. El. 12 (2001).
[43] T.R. Burkholder, J.T. Yustein, L. Andrews, J. Phys. Chem. 96 (1992) 10189.
[44] M. Nieminen, L. Niinistö, E. Rauhala, J. Mater. Chem. 6 (1996) 27.
[45] C. West, R. Mokaya, Chem. Mater. 21 (2009) 4080.
[46] G. Untila, T. Kost, A. Chebotareva, M. Zaks, A. Sitnikov, O. Solodukha, Semiconductors 42 (2008) 406.
[47] H. Lorenz, W. Jochum, B. Klötzer, M. Stöger-Pollach, S. Schwarz, K. Pfaller, S. Penner, Appl. Catal. A: Gen. 347 (2008) 34.
[48] O. Kazunari, Y. Tianchun, A. Yoshinobu, J. Vac. Sci. Technol. A: Vac. Surf. Films 12 (1994) 120.
[49] C.J. Carmalt, S.J. King, Coord. Chem. Rev. 250 (2006) 682.
[50] D.H. Kim, S.H. Yoo, T.-M. Chung, K.-S. An, H.-S. Yoo, Y. Kim, Bull. Korean Chem. Soc. 23 (2002) 225.
[51] Y. Kokubun, K. Miura, F. Endo, S. Nakagomi, Appl. Phys. Lett. 90 (2007) 031912.
[52] Y. Li, A. Trinchi, W. Wlodarski, K. Galatsis, K. Kalantar-Zadeh, Sens. Actuators B 93 (2003) 431.
[53] M. Valet, D.M. Hoffman, Chem. Mater. 13 (2001) 2135.
[54] L. Mîinea, S. Suh, S.G. Bott, J.-R. Liu, W.-K. Chu, D.M. Hoffman, J. Mater. Chem. 9 (1999) 929.
[55] S. Basharat, W. Betchley, C.J. Carmalt, S. Barnett, D.A. Tocher, H.O. Davies, Organometallics 26 (2007) 403.
[56] Y. Chi, T.-Y. Chou, Y.-J. Wang, S.-F. Huang, A.J. Carty, L. Scoles, K.A. Udachin, S.-M. Peng, G.-H. Lee, Organometallics 23 (2004) 95.
[57] S. Basharat, C.J. Carmalt, S.J. King, E.S. Peters, D.A. Tocher, Dalton Trans. (2004) 3475.
[58] S. Basharat, C.J. Carmalt, R. Palgrave, S.A. Barnett, D.A. Tocher, H.O. Davies, J. Organomet. Chem. 693 (2008) 1787.
[59] C.E. Knapp, L. Pemberton, C.J. Carmalt, D. Pugh, P.F. McMillan, S.A. Barnett, D.A. Tocher, Main Group Chem. 9 (2010) 31.
[60] C.E. Knapp, C.J. Carmalt, P.F. McMillan, D.A. Wann, H.E. Robertson, D.W.H. Rankin, Dalton Trans. (2008) 6880.
[61] G.E. Coates, R.G. Hayter, J. Chem. Soc. (1953) 2519.
[62] O.T. Beachley Jr., J.R. Gardinier, M.R. Churchill, L.M. Toomey, Organometallics 22 (2003) 1145.
[63] P. Wu, Y.-M. Gao, R. Kershaw, K. Dwight, A. Wold, Mater. Res. Bull. 25 (1990) 357.
[64] A. Ortiz, J.C. Alonso, E. Andrade, C. Urbiola, J. Electrochem. Soc. 148 (2001) F26.
[65] Q. Peng, D. Hojo, K.J. Park, G.N. Parsons, Thin Solid Films 516 (2008) 4997.
[66] B. Ballarin, G.A. Battiston, F. Benetollo, R. Gerbasi, M. Porchia, D. Favretto, P. Traldi, Inorg. Chim. Acta 217 (1994) 71.
[67] G.A. Battiston, R. Gerbasi, M. Porchia, R. Bertoncello, F. Caccavale, Thin Solid Films 279 (1996) 115.
[68] M. Hellwig, K. Xu, D. Barreca, A. Gasparotto, M. Winter, E. Tondello, R.A. Fischer, A. Devi, Eur. J. Inorg. Chem. (2009) 1110.
[69] J. Hao, M. Cocivera, J. Phys. D: Appl. Phys. 35 (2002) 433.
[70] Y. Ohya, J. Okano, Y. Kasuya, T. Ban, J. Ceram. Soc. Jpn. 117 (2009) 973.
[71] S. Chatterjee, S.R. Bindal, R.C. Mehrotra, J. Indian Chem. Soc. 53 (1976) 867.
[72] D.C. Bradley, H. Chudzynska, D.M. Frigo, M.B. Hursthouse, M.A. Mazid, Chem. Commun. (1988) 1258.
[73] C. Cantalini, W. Wlodarski, H.T. Sun, M.Z. Atashbar, M. Passacantando, S. Santucci, Sens. Actuators B 65 (2000) 101.
[74] L.A. Mîinea, S. Suh, D.M. Hoffman, Inorg. Chem. 38 (1999) 4447.
[75] S. Suh, D.M. Hoffman, J. Am. Chem. Soc. 122 (2000) 9396.
[76] K.J. Eisentraut, R.E. Sievers, J. Am. Chem. Soc. 87 (1965) 5254.
[77] L.A. Ryabova, Y.S. Savitskaya, J. Vac. Sci. Technol. 6 (1969) 934.
[78] V.F. Korzo, V.N. Chernyaev, Phys. Stat. Sol. A 20 (1973) 695.
[79] T. Maruyama, K. Fukui, J. Appl. Phys. 70 (1991) 3848.
[80] T. Tsuchiya, A. Watanabe, Y. Imai, H. Niino, I. Yamaguchi, T. Manabe, T. Kumagai, S. Mizuta, Jpn. J. Appl. Phys. 38 (1999) L1112.
[81] S. Reich, H. Suhr, B. Waimer, Thin Solid Films 189 (1990) 293.
[82] S. Venkat, N. Pammi, B.S. Sahu, N.-J. Seong, S.-G. Yoon, J. Vac. Sci. Technol. B 26 (2008) 909.
[83] G.E. Buono-Core, G. Cabello, B. Torrejon, M. Tejos, R.H. Hill, Mater. Res. Bull. 40 (2005) 1765.
[84] S.J. Bonyhady, C. Jones, S. Nembenna, A. Stasch, A.J. Edwards, G.J. McIntyre, Chem. Eur. J. 16 (2010) 938.
[85] M.S. Hill, P.B. Hitchcock, R. Pongtavornpinyo, Science 311 (2006) 1904.
[86] T.-Y. Chou, Y. Chi, S.-F. Huang, C.-S. Liu, A.J. Carty, L. Scoles, K.A. Udachin, Inorg. Chem. 42 (2003) 6041.
[87] R.B.H. Tahar, T. Ban, Y. Ohya, Y. Takahashi, J. Appl. Phys. 82 (1997) 865.
[88] A. Gurlo, M. Ivanovskaya, A. Pfau, U. Weimar, W. Göpel, Thin Solid Films 307 (1997) 288.
[89] J.-H. Lee, B.-O. Park, Surf. Coat. Technol. 184 (2004) 102.
[90] W.-Y. Chung, G. Sakai, K. Shimanoe, N. Miura, D.-D. Lee, N. Yamaoze, Sens. Actuators B 46 (1998) 139.
[91] W.-Y. Chung, G. Sakai, K. Shimanoe, N. Miura, D.-D. Lee, N. Yamaoze, Jpn. J. Appl. Phys. 37 (1998) 4994.
[92] W.-Y. Chung, G. Sakai, K. Shimanoe, N. Miura, D.-D. Lee, N. Yamaoze, Sens. Actuators B 65 (2000) 312.
[93] J. Tamaki, J. Niimi, S. Ogura, S. Konishi, Sens. Actuators B 117 (2006) 353.
[94] M.A. Flores-Mendoza, R. Castenedo-Perez, G. Torres-Delgado, J.M. Marín, O. Zelaya-Angel, Thin Solid Films 517 (2008) 681.
[95] M.A. Flores-Mendoza, R.C. Pérez, G.T. Delgado, O.Z. Angel, Thin Solid Films 518 (2009) 1114.
[96] T. Maruyama, K. Tabata, Jpn. J. Appl. Phys. 29 (1990) L355.
[97] T. Maruyama, K. Fukui, Thin Solid Films 203 (1991) 297.
[98] C.L.W. Ching, R.H. Hill, J. Vac. Sci. Technol. A 16 (1998) 897.
[99] D.D. Edwards, P.E. Folkins, T.O. Mason, J. Am. Ceram. Soc. 80 (1997) 253.
[100] A. Wang, N.L. Edleman, J.R. Babcock, T.J. Marks, M.A. Lane, P.R. Brazis, C.R. Kannewurf, J. Mater. Res. 17 (2002) 3155.
[101] C.E. Knapp, G. Hyett, I.P. Parkin, C.J. Carmalt, Chem. Mater., submitted for publication.
[102] B. Neumüller, Chem. Soc. Rev. 32 (2003) 50.
[103] A. Willner, A. Hepp, N.W. Mitzel, Dalton Trans. (2008) 6832.
[104] S. Basharat, C.E. Knapp, C.J. Carmalt, S.A. Barnett, D.A. Tocher, New J. Chem. 32 (2008) 1513.
[105] W. Uhl, I. Hahn, M. Koch, M. Layh, Inorg. Chim. Acta 249 (1996) 33.
[106] R.D. Schluter, H.S. Isom, A.H. Cowley, D.A. Atwood, R.A. Jones, F. Olbrich, S. Corbelin, R.J. Lagow, Organometallics 13 (1994) 4058.
[107] U. Werner, G. Rene, H. Ingo, S. Thomas, F. Walter, Eur. J. Inorg. Chem. 1998 (1998) 355.
[108] O.T. Beachley Jr., J.R. Gardinier, M.R. Churchill, Organometallics 19 (2000) 4544.
[109] O.T. Beachley Jr., J.R. Gardinier, M.R. Churchill, D.G. Churchill, K.M. Keil, Organometallics 21 (2002) 946.
[110] O.T. Beachley Jr., J.R. Gardinier, M.R. Churchill, L.M. Toomey, Organometallics 17 (1998) 1101.
[111] R.W. Chesnut, R.R. Cesati, C.S. Cutler, S.L. Pluth, J.A. Katzenellenbogen, Organometallics 17 (1998) 4889.
[112] Y. Shen, J. Han, H. Gu, Y. Zhu, Y. Pan, J. Organomet. Chem. 689 (2004) 3461.
[113] A.F. Lugo, A.F. Richards, Eur. J. Inorg. Chem. 13 (2010) 2025.
[114] W. Ziemkowska, A. Kubiak, S. Kucharski, R. Wozniak, R. Anulewicz-Ostrowska, Polyhedron 26 (2007) 1436.
[115] N.N. Chamazi, M.M. Heravi, B. Neumüller, Z. Anorg. Allg. Chem. 633 (2007) 709.
[116] S.V. Suslova, N.Y. Turova, A.S. Mityaev, A.V. Kepman, S. Gohil, Russ. J. Inorg. Chem. 53 (2008) 665.
[117] K. Utsunomiya, Bull. Chem. Soc. Jpn. 44 (1971) 2688.
[118] H.R. Hoveyda, V. Karunaratne, S.J. Rettig, C. Orvig, Inorg. Chem. 31 (1992) 5408.
[119] S. Daniele, D. Tcheboukov, L.G. Hubert-Pfalzgraf, S. Lecocq, Inorg. Chem. Commun. 5 (2002) 347.
[120] D.W. Johnson, J. Xu, R.W. Saalfrank, K.N. Raymond, Angew. Chem. Int. Ed. 38 (1999) 2882.
[121] M. Albrecht, S. Schmid, M. deGroot, P. Weis, R. Fröhlich, Chem. Commun. (2003) 2526.
[122] M. Albrecht, S. Dehn, R. Fröhlich, Angew. Chem. Int. Ed. 45 (2006) 2792.
[123] S.V. Suslova, K.V. G, S. Gohil, N.Y. Turova, Eur. J. Inorg. Chem. 2007 (2007) 5182.
[124] R. Saalfrank, H. Maid, A. Scheurer, F. Heinemann, R. Puchta, W. Bauer, D. Stern, D. Stalke, Angew. Chem. Int. Ed. 47 (2008) 8941.